Molecular Therapy
Methods & Clinical Development
Original Article

mRNA vaccines encoding membrane-anchored RBDs of SARS-CoV-2 mutants induce strong humoral responses and can overcome immune imprinting

Hareth A. Al-Wassiti,[1] Stewart A. Fabb,[1] Samantha L. Grimley,[2] Ruby Kochappan,[1] Joan K. Ho,[1] Chinn Yi Wong,[2] Chee Wah Tan,[3] Thomas J. Payne,[1] Asuka Takanashi,[1] Chee Leng Lee,[1] Rekha Shandre Mugan,[1] Horatio Sicilia,[1] Serena L.Y. Teo,[1] Julie McAuley,[2] Paula Ellenberg,[2] James P. Cooney,[4,5] Kathryn C. Davidson,[4] Richard Bowen,[6] Marc Pellegrini,[4] Steven Rockman,[2,7] Dale I. Godfrey,[2] Terry M. Nolan,[2] Lin-fa Wang,[3] Georgia Deliyannis,[2] Damian F.J. Purcell,[2] and Colin W. Pouton[1]

[1]Monash Institute of Pharmaceutical Sciences, Monash University, Parkville, VIC 3052, Australia; [2]Peter Doherty Institute for Infection and Immunity, and Department of Infectious Diseases, University of Melbourne, Melbourne, VIC 3000, Australia; [3]Duke-NUS Medical School, Singapore 169857, Singapore; [4]Walter and Eliza Hall Institute, Parkville, VIC 3052, Australia; [5]Department of Medical Biology, University of Melbourne, Parkville, VIC 3052, Australia; [6]Biomedical Sciences, Colorado State University, Fort Collins, CO 80523, USA; [7]Seqirus, Parkville, VIC 3052, Australia

We investigated mRNA vaccines encoding a membrane-anchored receptor-binding domain (RBD), each a fusion of a variant RBD, the transmembrane (TM) and cytoplasmic tail fragments of the severe acute respiratory syndrome coronavirus 2 (SARS-CoV-2) spike protein. In naive mice, RBD-TM mRNA vaccines against SARS-CoV-2 variants induced strong humoral responses against the target RBD. Multiplex surrogate viral neutralization (sVNT) assays revealed broad neutralizing activity against a range of variant RBDs. In the setting of a heterologous boost, against the background of exposure to ancestral whole-spike vaccines, sVNT studies suggested that BA.1 and BA.5 RBD-TM vaccines had the potential to overcome the detrimental effects of immune imprinting. A subsequent heterologous boost study using XBB.1.5 booster vaccines was evaluated using both sVNT and authentic virus neutralization. Geometric mean XBB.1.5 neutralization values after third-dose RBD-TM or whole-spike XBB.1.5 booster vaccines were compared with those after a third dose of ancestral spike booster vaccine. Fold-improvement over ancestral vaccine was just 1.3 for the whole-spike XBB.1.5 vaccine, similar to data published using human serum samples. In contrast, the fold-improvement achieved by the RBD-TM XBB.1.5 vaccine was 16.3, indicating that the RBD-TM vaccine induced the production of antibodies that neutralize the XBB.1.5 variant despite previous exposure to ancestral spike protein.

INTRODUCTION

Waves of coronavirus infections resulting from the coronavirus disease 2019 (COVID-19) pandemic are caused by mutants of the severe acute respiratory syndrome coronavirus 2 (SARS-CoV-2) that evade humoral immunity previously acquired by way of either vaccination or viral infection. Although vaccination with an ancestral SARS-CoV-2 whole-spike vaccine provides protection against serious illness,[1,2] boosting immunity with ancestral vaccines is ineffective at preventing infection by Omicron variants.[3–6] To address this shortcoming, bivalent mRNA spike vaccines were introduced that initially encoded BA.1, and later BA.5, spike proteins in addition to the ancestral spike protein.[7,8] In 2023, monovalent vaccines against XBB.1.5 were approved for use.[9] These are soon to be replaced by vaccines targeted against the KP.2 variant, which has been in circulation in 2024. Unfortunately, the effectiveness of the modified whole-spike vaccines to prevent infection by Omicron variants seems to be compromised by the phenomenon of immune imprinting,[10,11] a recognized problem that can limit the effectiveness of vaccination as viruses mutate.[12,13] Evasive variant coronaviruses acquire mutations in the receptor-binding domain (RBD), which allow the virus to evade antibodies that bind strongly to the ancestral RBD.[14–17] Individuals who have been exposed to the ancestral spike protein are primed to produce antibodies that bind to a range of different epitopes within this large 1,273-amino acid protein. Subsequent vaccination with mRNA, encoding Omicron variants of whole-spike protein, results in a significant boost in the production of antibodies against ancestral epitopes, rather than focusing the immune system on the induction of new antibodies that improve the ability of polyclonal antiserum to neutralize the variant RBD.[18]

Received 30 October 2023; accepted 12 November 2024;
https://doi.org/10.1016/j.omtm.2024.101380.

Correspondence: Colin W. Pouton, Monash Institute of Pharmaceutical Sciences, Monash University, 381 Royal Parade, Parkville, VIC 3052, Australia.
E-mail: colin.pouton@monash.edu

Crown Copyright © 2024 Published by Elsevier Inc. on behalf of The American Society of Gene and Cell Therapy.
This is an open access article under the CC BY-NC-ND license (http://creativecommons.org/licenses/by-nc-nd/4.0/).

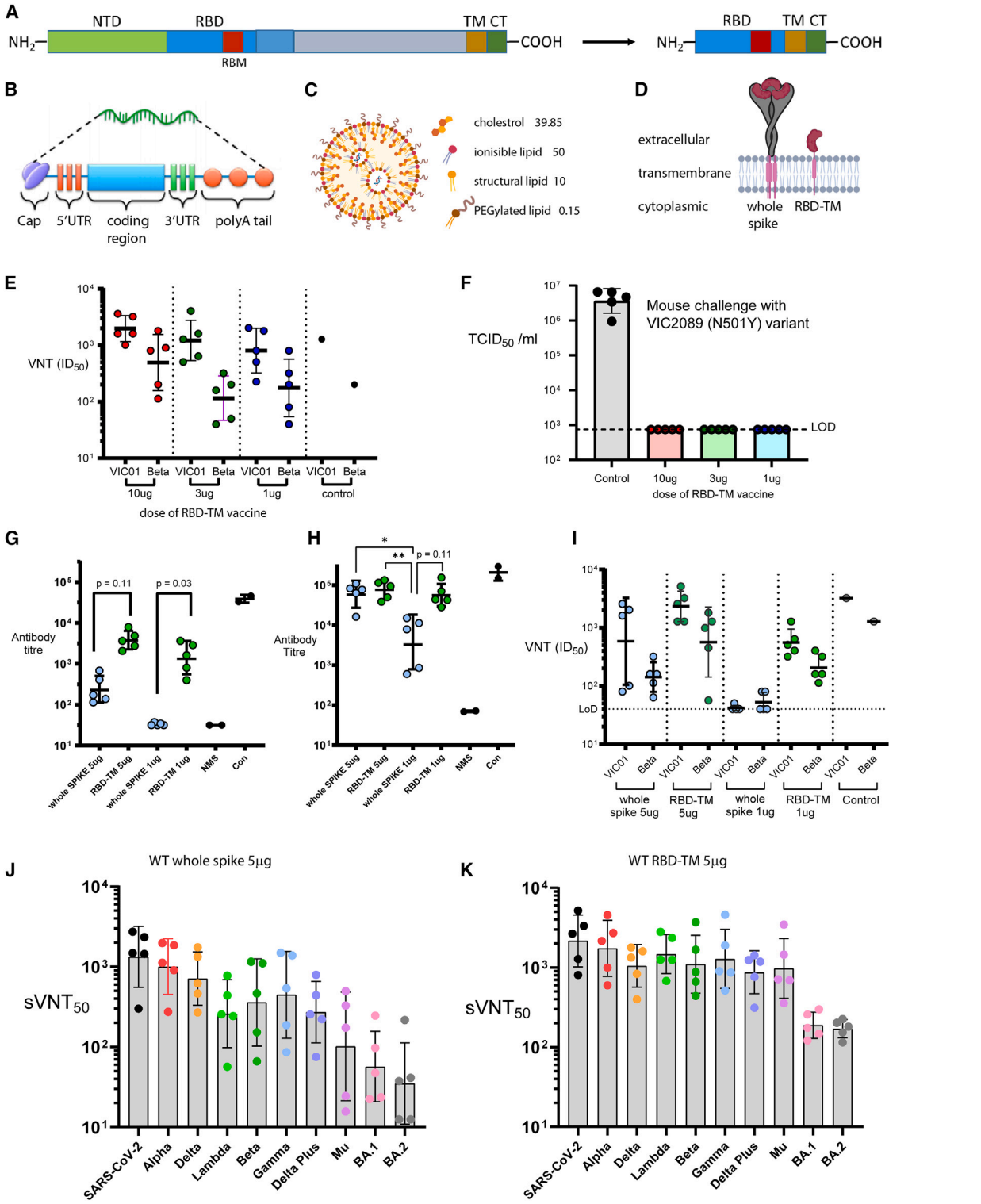

Figure 1. Comparison of immunogenicity induced by RBD-TM mRNA and whole-spike mRNA vaccines

(A) Schematic diagram comparing whole SARS-CoV-2 spike protein (1,273 amino acids) with the RBD-TM construct (328 amino acids). (B) Common features of the mRNA vaccines used in this study. We used TriLink CleanCap reagent to produce the Cap1 structure, and used a 125 nucleotide polyA tail. The UTRs were designed *de novo* with reference to known sequences. (C) General features of the LNP delivery system used. The identities and concentrations of ionizable and PEGylated lipids are described in the

(legend continued on next page)

To protect aging and vulnerable populations from future infections by evasive mutants, next-generation COVID vaccines will need to overcome the problem of immune imprinting. To address this need we developed an alternative platform (RBD-transmembrane [TM]) designed to focus immune responses on new antigenic epitopes resulting from mutations in the RBD. Our hypothesis is that by deleting much of the whole-spike protein (the N-terminal domain, the remainder of the S1 region and the majority of the S2 region), the RBD-TM will avoid boosting of non-neutralizing antibodies that bind to the deleted regions of the whole-spike protein. The protein coding sequences of our RBD-TM mRNA vaccines are constructed by fusing a cDNA encoding the appropriate RBD domain by way of a short spacer to cDNA encoding the ancestral TM and cytoplasmic tail (CT). The protein sequence of the ancestral RBD-TM fusion protein and the mRNA encoding this protein are shown in Figure S1. The complete RBD-TM mRNAs have similar design features to those used in the approved whole-spike vaccines,[1,19,20] as described in the materials and methods section, and are formulated in lipid nanoparticles (LNPs) in an analogous manner.

In this article, we describe (1) our initial preclinical studies comparing ancestral RBD-TM vaccine with ancestral whole-spike vaccine; (2) the development of a Beta variant (K417N, E484K, N501Y) RBD-TM vaccine, which was later manufactured for human use and has undergone evaluation in a phase 1 clinical trial; (3) preclinical experiments in naive mice to test immune responses to a range of variant RBD-TM vaccines, including Delta, Delta-plus, Kappa, Omicron BA.1, BA.5, and XBB.1.5 vaccines; and (4) experiments in mice to simulate real-world vaccination against a background of exposure to ancestral SARS-CoV-2 whole-spike protein. The study shows that RBD-TM mRNAs provide an adaptable platform for the production of prophylactic vaccines, which we hypothesize has the potential to protect elderly and vulnerable individuals from infection by emerging coronavirus variants. A phase 1 clinical study of the Beta RBD-TM mRNA as a fourth-dose booster vaccine has been completed. Interim data from the trial are now available in a separate article.[21]

RESULTS

Immunogenicity induced by ancestral RBD-TM and whole-spike mRNA vaccines

The components of the RBD-TM mRNA COVID-19 vaccine platform are shown schematically in Figures 1A–1D and are described in the materials and methods section and in Figures S1 and S2. The RBD-TM mRNA is 28% of the length of whole-spike mRNA (Figure 1A) and is designed to be expressed as a membrane-anchored monomeric RBD (Figure 1D). Unless otherwise described, this vaccine was delivered in an LNP with low content (0.15%–0.25 mol%) of PEGylated lipid (Figure 1C). An initial prime and boost experiment was carried out at doses of 1, 3, or 10 μg mRNA to determine whether the ancestral SARS-CoV-2 RBD-TM vaccine induced immunity in naive BALB/c mice. Virus neutralization (VNT) studies using an early isolate of the ancestral SARS-CoV-2 virus (VIC01) or a Beta variant virus indicated that strong antibody (Ab) responses were induced at doses of mRNA greater than 1 μg (Figure 1E). Neutralization titers determined using the Beta variant virus were consistently lower at all three doses of mRNA. At the dose of 3 μg, which we subsequently established is adequate for vaccination in mice, ID_{50} values were 1,621 ± 644 against VIC01 and 154 ± 52 against the Beta isolate (mean ± SEM, $n = 5$, geometric means were 1,222 and 115, respectively). When the mice were challenged (see materials and methods) on day 65 with VIC2089, a SARS-CoV-2 variant that had acquired the N501Y mutation, also found in the Alpha variant, all three doses of ancestral RBD-TM vaccine protected the lungs from infection (Figure 1F). To compare the immune responses of mice vaccinated with either RBD-TM or whole-spike mRNAs, we carried out prime and boost vaccination at either 1 or 5 μg mRNA. Ancestral RBD-specific Ab titers determined 3 weeks after the prime or boost (i.e., day 21 or 42) are shown in Figures 1G and 1H. VNT by serum samples collected on day 42 was evaluated using VIC01 or the Beta variant (Figure 1I). At each dose, the RBD-TM was more potent than whole spike, although the Ab titers had reached a limiting value for either vaccine at the 5-μg dose (Figure 1H). The high potency of the RBD-TM is possibly because the RBD-TM mRNA encodes 3.6-fold more RBD units than the same mass of whole-spike mRNA. ID_{50} values for neutralization of VIC01 after two 5-μg doses of whole-spike or RBD-TM mRNA were 1,277 ± 507 and 2,693 ± 714 (mean ± SE, $n = 5$, geometric means 583 and 2,334), respectively (Figure 1I). This difference was not significant, probably due to lack of statistical power, or because both vaccines were close to saturating the immune response against the target RBD at the 5-μg dose. The higher activity of antisera against VIC01 after two doses of RBD-TM versus whole spike at the 1-μg and 3-μg doses were not significant when tested using non-parametric methods. The VNT studies suggested showed that a dose of 1μg whole-spike mRNA failed to induce a robust

materials and methods section. (D) Cartoon representation of the proteins resulting from translation of the whole-spike and RBD-TM mRNAs. (E) Neutralization of infection of Vero cells by serum samples from mice vaccinated intramuscularly (IM) with WT SARS-CoV-2 RBD-TM vaccine. BALB/c mice were vaccinated on day 0 and 21 with either 1, 3, or 10 μg mRNA. Serum samples were collected on day 42. Viral strains used were the VIC01 isolate of WT SARS-CoV-2 or the Beta B.1.351 variant. The control serum was obtained by pooling serum collected on day 56 after vaccination of BALB/c mice with 30 μg whole-spike vaccine. (F) Viral titers in lungs of the mice from (E) 3 days after challenge with an N501Y mutant of SARS-CoV-2 (hCoV-19/Australia/VIC2089/2020) on day 65, 44 days after the second dose of vaccine. The titer of infectious virus ($TCID_{50}$) in the lungs of individual mice were determined by titrating lung homogenate supernatants on Vero cell monolayers and measuring viral cytopathic effect 5 days later. Control animals were unvaccinated aged-matched BALB/c mice. (G and H) RBD-specific Ab titers determined by ELISA in mouse serum samples after either 1- or 5-μg doses IM on days 0 and 21 of either WT whole-spike or WT RBD-TM vaccines. Ab titers were determined on day 21 (G) or on day 42 (H). (I) Neutralization of infection of Vero cells, by VIC01 or Beta strains of virus, by the day 42 serum samples used for ELISA studies in (H) (geometric mean ± geometric SD; $n = 5$). (J and K) sVNT studies using multiplexed variant RBD-beads indicating relative neutralization of SARS-CoV-2 variants by the serum samples as used in (I) after doses of either 5 μg of WT whole-spike (J) or 5 μg of WT RBD-TM (K) vaccines. The half-maximal inhibitory dilution ($sVNT_{50}$) is indicated for each serum sample. Horizontal lines show geometric mean; error bars show geometric SD ($n = 5$ mice); statistical analysis shown in (G and H) used the Kruskal-Wallis test with Dunn's multiple comparisons test, $^{*}p < 0.05$, $^{**}p < 0.01$. For all panels, unless shown, multiple comparisons were not statistically significant.

neutralizing Ab response (Figure 1I). Surrogate viral neutralization (sVNT) studies were carried out in multiplex to evaluate the ability of mouse serum to inhibit of binding of a range of RBD variants to human angiotensin-converting enzyme 2(ACE2) (Figures 1J and 1K). Details of the specific mutations in each RBD are shown in Figure S3. The 5-μg doses of whole-spike vaccine induced $sVNT_{50}$ values of greater than 100 for all variants other than Mu and Omicron BA.1 and BA.2 variants. The same mass of RBD-TM vaccine induced consistently higher $sVNT_{50}$ values for all variants with titers above 100 for the two Omicron variants. The mean percent neutralization data for four dilutions of serum samples are shown in Figure S4.

Development of a beta variant RBD-TM mRNA vaccine for clinical evaluation

In mid 2021, we began preparing for clinical evaluation of the RBD-TM platform by developing a vaccine against the Beta variant of SARS-CoV-2. Before the emergence of Omicron in late 2021, Beta was the variant of concern that had acquired the most consistent ability to evade immunity induced by ancestral vaccines.[22] Figure 2 outlines the preclinical data supporting the development of the clinical Beta RBD-TM vaccine. Prime and boost studies were carried out in BALB/c mice vaccinated with doses between 0.1 and 10 μg mRNA. Ab titers on day 21 after the priming dose suggested that the dose-response relationship was close to linear over the range of 0.1–3 μg against the target Beta RBD or ancestral RBD (Figures 2A and 2B). Titers were consistently higher against the target Beta variant and could be assessed using ELISA against either Beta RBD or ancestral RBD-coated plates. Ab titer was below 10^3 after 0.1-μg doses, even after the boost dose at day 42 or 56 (Figures 2C and 2D). Serum collected on day 56 was evaluated by VNT using ancestral VIC01 or the Beta variant (Figure 2E). A 3-μg dose induced adequate protection, producing mean VNT(ID_{50}) values of 723 ± 166 and 283 ± 53 (mean ± SEM, n = 5, geometric means 611 and 260) against Beta and VIC01, respectively. The higher activity against the target variant was not significantly different at n = 5. In a second study using a different batch of vaccine, we extended the dose range to 10 μg. Ab titers and VNT data at day 56 are shown in Figures 2F and 2G.

The data are in good agreement with the earlier experiments and shows that Ab responses were not enhanced by increasing the dose from 3 to 10 μg. Multiplex sVNT studies indicated that ACE2 binding of all RBD variants tested was strongly inhibited by serum samples collected on day 56 after two 3-μg doses of Beta RBD-TM, suggesting that the Beta vaccine induced broad spectrum activity. The highest $sVNT_{50}$ values were observed against the Beta, Gamma, and Mu variant RBDs, all of which share the E484K mutation. Inspection of the mean percent neutralization data at various dilutions (Figure S5) revealed that, although protection against Beta, ancestral, and Alpha RBDs was similar at doses of 3 and 10 μg, there was a noticeable increase in inhibition of ACE2-binding by other variants, including Omicron BA.1 and BA.2 at the higher dose, suggesting that broader spectrum activity could be gained by using higher doses of RBD-TM vaccines.

In preparation for manufacture of the clinical Beta RBD-TM vaccine, we considered whether our LNP formulation would perform adequately in comparison with those used in the approved mRNA vaccines (see discussion for more detail). To evaluate this, we tested immunity induced by 3 μg of our Beta RBD-TM mRNA in each of four alternative LNP formulations. The formulations differed in the choice of ionizable lipid (50 mol% MC3 or ALC-0315) and also in the mole% of PEGylated lipid used (1.5% or 0.15% DMG-PEG). Our mRNA vaccines were usually formulated using MC3 and 0.15 mol% DMG-PEG (see the discussion). A more standard LNP formulation is MC3 with 1.5 mol% DMG-PEG. By swapping out MC3 for ALC-0315, we tested a formulation (50 mol% ALC-0315 and 1.5% DMG-PEG) which was closer to that used in the BioNTech/Pfizer COVID vaccine (Comirnaty), which contains 46.3 mol% ALC-0315 and 1.6 mol% of the PEGylated lipid ALC-0159. We also tested the 50 mol% ALC-0315 formulation with 0.15% DMG-PEG. A comparison of the four LNP formulations tested is shown in Figure 3. All four formulations produced strong immune responses. Ab titers for the ALC-0315/1.5% DMG-PEG formulation were significantly higher than for the corresponding 0.15% DMG-PEG formulation when tested against ancestral RBD-coated plates (Figures 3A and 3C). The Ab titers induced by the two 0.15% DMG-PEG formulations were not significantly different when tested against either ancestral RBD-coated plates (Figures 3A and 3C) or target Beta RBD-coated plates (Figures 3B and 3D). VNT studies confirmed that all four formulations induced serum samples with ID_{50} values that were not significantly different (Figure 3E). In all cases, protection against viral infection seemed to be more effective against the target Beta strain, although the differences were not statistically significant. Mice were challenged with live Beta SARS-CoV-2 virus. Viral titers in the nasal turbinates or lungs were evaluated on day 3. All four vaccines protected mice from challenge by live virus (Figures 3F and 3G). To extend our evaluation of alternative formulations and comparison of the RBD-TM vaccine with whole-spike vaccines, we vaccinated mice with either ancestral RBD-TM mRNA or whole-spike mRNA at doses of 1 or 5 μg, but this time using LNPs containing ALC-0315, cholesterol, distearoylphosphatidylcholine (DSPC), and DMG-PEG2000 in the mole ratio of 46.3:42.7:9.4:1.6. This formulation differs from the formulation used for Comirnaty only in the identity of the PEGylated lipid. Ab titers and VNT data are shown in Figure S6. The data consistently suggests that, on the basis of mass, the RBD-TM vaccine is more potent than whole-spike vaccine, although the differences between the two vaccines using groups of five mice were not statistically different. Both Ab titers and VNT data compared favorably with the analogous data obtained after vaccination with our MC3 50 mol%/DMG-PEG 0.15 mol% formulation (Figure 1), again giving confidence that we could prepare an RBD-TM vaccine for clinical evaluation using the latter formulation.

Activity of the beta RBD-TM mRNA vaccine in Syrian hamsters and Sprague Dawley rats

A hamster challenge study was carried out according to the methods described in the Supplementary data file (Figure S7). This study was carried out in parallel with the evaluation of a protein Beta RBD-Fc

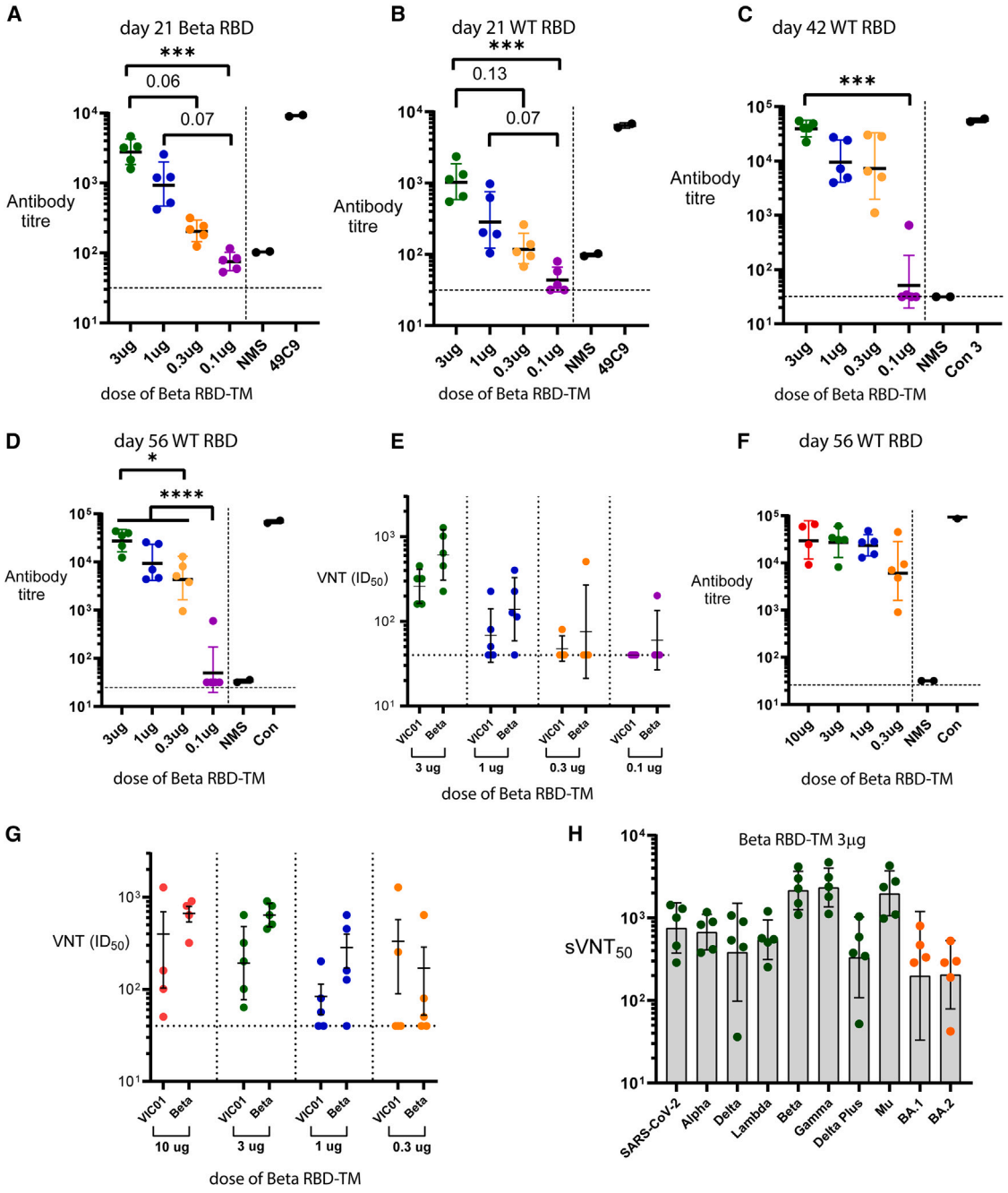

Figure 2. Immunogenicity of Beta RBD-TM mRNA vaccine as a function of dose

(A–D) RBD-specific Ab titers in mouse serum after doses of Beta RBD-TM vaccine administered IM on days 0 and 21. Titers on day 21 against Beta RBD (A) and titers against WT RBD on day 21 (B), day 42 (C), or day 56 (D). NMS, normal mouse serum; 49C9, control antiserum; control, serum from mice treated with 30 µg native mRNA vaccine. Horizontal lines show the geometric mean; error bars show the geometric SD (n = 5 mice). Statistical analysis Kruskal-Wallis test with Dunn's multiple comparisons test, $^{*}p < 0.05$, $^{**}p < 0.01$, $^{***}p < 0.001$. (E) Neutralization of infection of Vero cells by serum samples from mice vaccinated IM with various doses of Beta RBD-TM vaccine. Neutralization of WT VIC01 or a Beta variant are shown. (F and G) RBD-specific Ab titers (F) and VNT (G) in mouse serum at day 56 after two doses of Beta RBD-TM vaccine (day 0 and day 21) in an experiment to extend the dose range to 10 µg. (H) sVNT study using multiplexed variant RBD-beads on day 56 after 3-µg doses of Beta RBD-TM vaccine. Half-maximal inhibitory dilution ($sVNT_{50}$) is indicated for each serum sample. Horizontal lines show geometric mean; error bars show geometric SD (F–H) (n = 5 mice). For all panels, unless shown, multiple comparisons were not statistically significant.

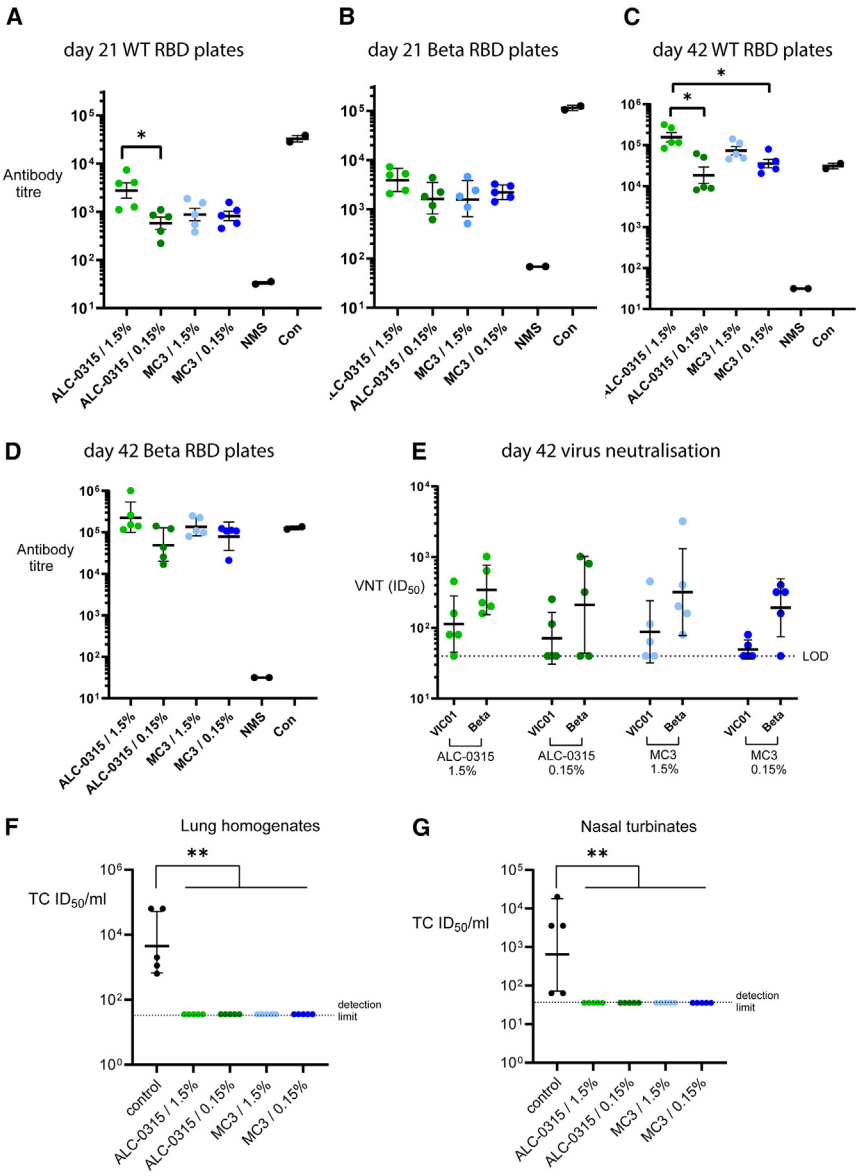

Figure 3. Immunogenicity and protective efficacy of the Beta RBD-TM mRNA vaccine administered in different LNP formulations

(A–D) WT (A, C) or Beta (B, D) RBD-specific Ab titers in Balb/c mouse serum 21 days after a single dose (A, B) or on day 42 (C and D), 21 days after a second dose of 3 μg Beta RBD-TM mRNA formulated in each of four LNPs. The LNPs were formulated with either of two ionizable lipids (ALC-0315 at 46.3 mol% or DLin-MC3-DMA at 50 mol%) with either 1.5 mol% or 0.15 mol% DMG-PEG2000. Horizontal bars show the geometric mean; error bars show the geometric SD (n = 5 mice). Statistical analysis Kruskal-Wallis test with Dunn's multiple comparisons test, *p < 0.05. (E) Half-maximal VNT titers determined against VIC01 or Beta SARS-CoV-2 using the day 42 serum samples used in (C and D). Horizontal bars show the geometric mean; error bars show the geometric SD. (F and G) Viral titers in lungs (F) or nasal turbinates (G) of the mice from (A–E) 3 days after aerosol challenge with a Beta variant (B.1.351) of SARS-CoV-2 on day 65, 44 days after the second dose of vaccine. Control mice were untreated aged-matched Balb/c mice. Horizontal lines show geometric mean titers in control mice. Titers in all four groups of vaccinated mice were below the limit of detection. Results reported in Figures 1, 2, 4, 5, and 6 were obtained after the administration of vaccines in a single LNP formulation using 50 mol% DLin-MC3-DMA and 0.15% DMG-PEG2000. For all panels, unless shown, multiple comparisons were not statistically significant.

adjuvanted by coadministration with MF59.[23] At doses of 3, 10, or 30 μg, the RBD-TM vaccine was unable to induce full protection against infection with either ancestral or Beta SARS-CoV-2. A marginal reduction in viral titers in oropharyngeal swabs was observed, but not in hamster lung tissue. With the protein Beta RBD-Fc vaccine, we observed partial protection in hamsters rather than the complete protection seen in mice. These data suggest that hamsters may not respond well to RBD vaccines, an observation supported by Zhang et al.[24] Given that the RBD-TM mRNA vaccine has been shown to be active in humans,[25] no further studies on hamsters have been conducted. A toxicity study to support the development of the clinical Beta RBD-TM vaccine was carried out in Sprague-Dawley rats by an independent contract research organization (Figure S8). For toxicity purposes the rats received three doses of 50 μg Beta RBD-TM mRNA, which was later used as the highest dose in the clinical study.[21] High mean Ab titers of greater than 10^5 were present in the rat serum from after three doses of RBD-TM vaccine in either male (n = 15) or female (n = 15) rats (Figure S8). The independent toxicity study did not raise any concerns and was consistent with expectations for mRNA-LNP vaccines administered by the intramuscular route. Three injections, each of 50 μg mRNA, were administered on days 1, 22, and 43. Mild to moderate acute effects, limping, and a palpably firm injection site were observed for 24–28 h after the injection, which were attributed to the treatment but resolved in all instances. At the completion of the treatment period terminal examinations were conducted on study days 44 or 45 for 10 male and 10 female rats from each treatment group. Additional rats, five per sex, from all groups were allowed a treatment-free recovery period of a further 2 weeks before necropsy on study day 56. At study days 44 or 45, there was a significant increase in neutrophils, eosinophils, and basophils for both male and female rats treated with the Beta RBD-TM mRNA vaccine. This increase was considered to be an effect of treatment but not considered adverse as the vaccine was expected to produce an immunological response and the findings showed evidence of reversibility on study day 56. On study day 44 or 45, there was an increase in alanine aminotransferase (ALT), alkaline

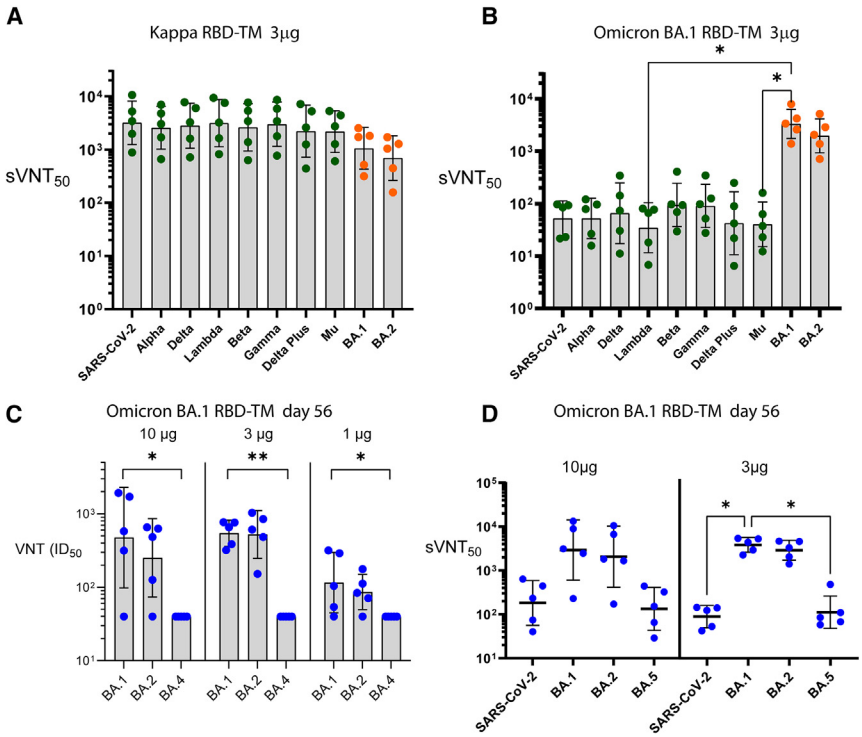

Figure 4. Immunogenicity of Kappa and Omicron BA.1 RBD-TM mRNA vaccines

(A and B) sVNT study of BALB/c mouse serum using multiplexed variant RBD-beads on day 56, after two 3-μg doses (days 0 and 21) of either Kappa (A) or Omicron BA.1 (B) RBD-TM vaccines. (C) Half-maximal VNT titers determined against naturally occurring Omicron BA.1, BA.2 and BA.4 variants of SARS-CoV-2 in serum collected on day 56 after two doses (day 0 and 21) of Omicron BA.1 RBD-TM mRNA vaccine administered at doses of 1, 3, or 10 μg mRNA. BA.4 VNT was below the effective limit of detection of the assay for all three doses. (D) sVNT study of BALB/c mouse serum on day 56 after 3- or 10-μg doses of Omicron BA.1 RBD-TM mRNA using WT SARS-CoV-2, BA.1, BA.2 or BA.5-RBD-coated beads. Half-maximal inhibitory dilution ($sVNT_{50}$ or $VNT(ID_{50})$) is indicated for each serum sample. Horizontal lines or bars show the geometric mean; error bars show the geometric SD (in A–D) ($n = 5$ mice). Statistical analysis Kruskal-Wallis test with Dunn's multiple comparisons test, $^{*}p < 0.05$, $^{**}p < 0.01$. For all panels, unless shown, multiple comparisons were not statistically significant.

phosphatase (ALP), and aspartate aminotransferase (AST) concentrations in Beta RBD-TM mRNA-treated female rats relative to the saline-treated control group, which resolved by study day 56. These increases in ALT, ALP, and AST concentrations were not correlated with any microscopic findings, and while associated with the SARS-CoV-2 RBD mRNA treatment, were considered to not be adverse. Focal or multifocal, minimal to marked, mixed cell inflammation of the injection site was observed in virtually all animals. The inflammation and its associated features primarily affected the skeletal muscle, with occasional involvement of the subcutaneous tissue, and correlated with macroscopic findings including firmness, paleness, yellow and/or red discoloration, mass, and irregular areas. The report concluded that treatment with 50 μg RBD-TM mRNA in the LNP formulation was well tolerated with the observed effects of treatment consistent with intramuscular vaccine administration and showing evidence of reversibility.

VNTs and multiplex sVNTs reveal breadth of immunity induced by alternative RBD-TM vaccines

The RBD-TM platform can be rapidly tuned to target emerging variants with mutations in the RBD domain. We vaccinated naive mice with a range of alternative RBD-TM vaccines targeting Delta, Delta-plus, Kappa, or Omicron BA.1. Data are shown in Figures 4 and S9–S11. The Delta variant vaccine induced serum with a spectrum of activity against other variants that were in accordance with our expectations. The mean percent neutralization was greatest against the Delta RBD; strong against ancestral and Alpha; weaker against Beta, Gamma, and Mu; and weaker still against Omicron BA.1 and BA.2 (Figure S9). The Delta-plus vaccine showed tighter neutralization of early variants but was weaker than Delta against BA.1 and BA.2 (Figure S9).

The Kappa variant RBD-TM proved to be a remarkably broad-spectrum vaccine. After two doses of the Kappa vaccine, the mouse serum samples strongly inhibited ACE2 binding of all early variants, including Omicron BA.1 and BA.2 (Figure 4A). In contrast, the Omicron BA.1 RBD-TM vaccine produced strong inhibition of BA.1 and BA.2 RBDs but weak activity against all other earlier variants (Figure 4B). When Omicron BA.4 and BA.5 emerged, we tested the serum samples from BA.1 RBD-TM vaccinated mice using BA.4 virus in VNT studies (Figure 4C) and the BA.4/BA.5 RBD (which is identical) in sVNT studies (Figure 4D). The data from these assays were aligned in that the BA.1 vaccine induced serum samples that could neutralize BA.1 and BA.2 but not BA.4/BA.5. The broader neutralizing capacity of higher doses of vaccine can be observed again in the estimates of neutralizing activity of serum from mice after two doses of 3 or 10 μg BA.1 RBD-TM vaccine (Figure S10). No further increases in activities after doses of 10 μg were evident against BA.1 or BA.2 RBDs, but the mean percent neutralization values at each dilution were higher against the early pre-Omicron variants after two 10-μg doses versus two 3-μg doses. Recently, our multiplex sVNT assay was extended to include beads coupled with the RBDs of XBB, XBB.1.5, and SARS-CoV-1. The remarkable breadth of activity of the Kappa RBD-TM was further demonstrated, showing induction of strong responses even at a dose of 0.3 μg against BA.5, XBB, and XBB.1.5 and encouraging activity against SARS-CoV-1 at 3 μg (Figure S11).

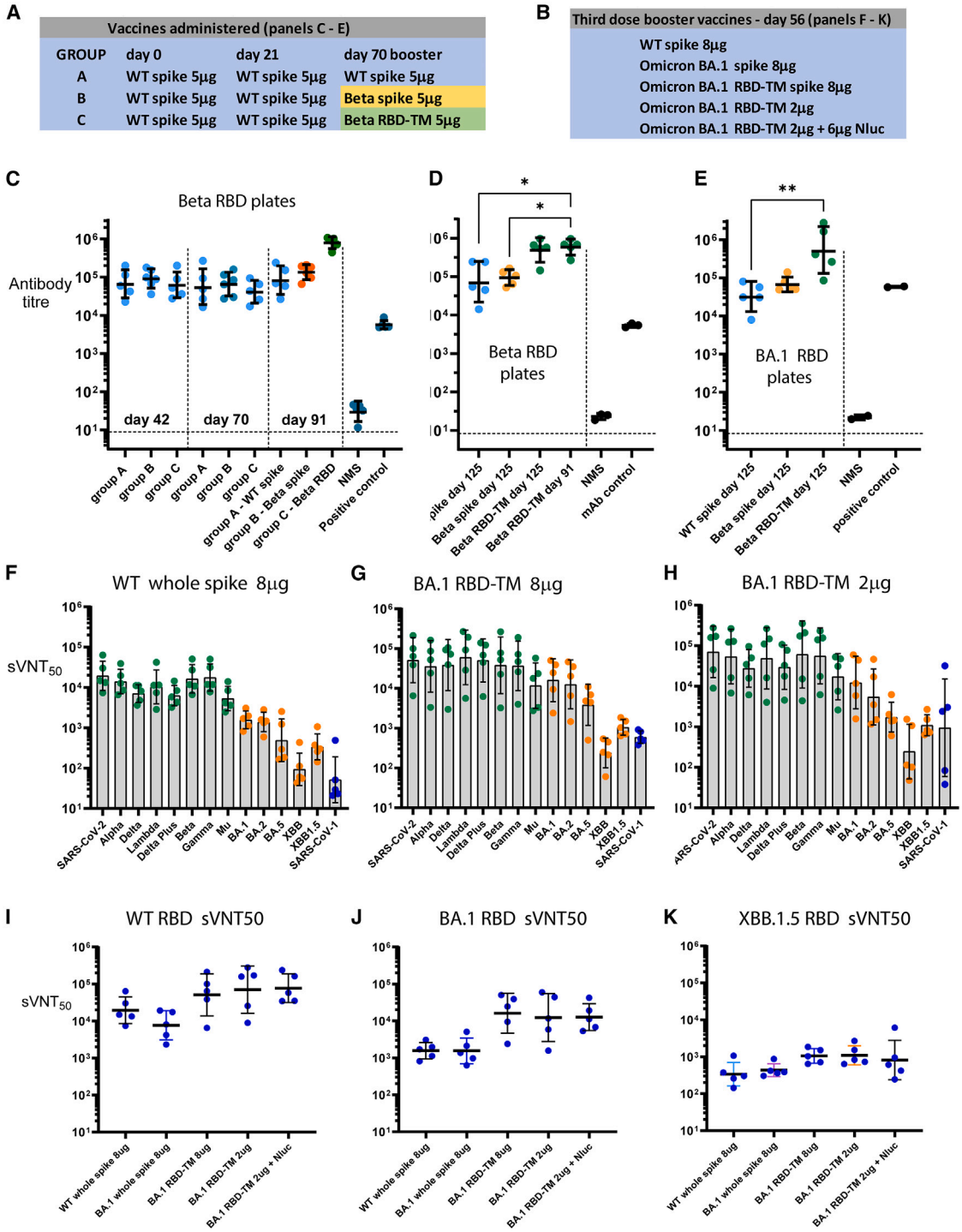

Figure 5. Heterologous boost studies using Beta or Omicron BA.1 RBD-TM vaccines after exposure to WT whole-spike mRNA vaccine

(A and B) Vaccines administered to each group of mice in heterologous boost tests of Beta (A) or Omicron BA.1 (B) RBD-TM vaccines. (A) Relates to data shown in (C–E). (B) Relates to the data shown in panels (F–K) and lists the alternative vaccines administered on day 56 after two 8-µg doses of WT spike vaccine administered on days 0 and 21. (C) Beta RBD-specific Ab titers in BALB/c mouse serum samples at day 42 and day 70 after two 5-µg doses (days 0 and 21) of WT whole-spike mRNA vaccine, and on day 91 after one of three alternative booster doses administered on day 70. (D and E) Beta RBD-specific (D) and Omicron BA.1 RBD-specific Ab titers in mouse serum samples from the three groups on day 125. Horizontal bars show geometric mean; error bars show geometric SD (n = 5 mice); statistical analysis Kruskal-Wallis test with Dunn's multiple

(legend continued on next page)

Heterologous boost experiments in mice demonstrate that RBD-TM mRNA vaccines can overcome immune imprinting

In early heterologous boost experiments we vaccinated mice with two 5-μg doses of ancestral whole-spike mRNA, subsequently administering a third booster vaccine with 5-μg doses of mRNA encoding either ancestral whole spike, Beta whole spike, or Beta RBD-TM. The protocol for these experiments is shown in Figure 5A. Figure 5C shows that all groups of animals had consistent Ab titers after the first and second doses of ancestral whole spike. On day 91, 3 weeks after the boost, there was evidence of a slight elevation in titers of Beta RBD-specific antibodies after boosting with the Beta whole-spike vaccine and a significant elevation, maintained until day 125, after boost with the Beta RBD-TM vaccine (Figure 5D). Omicron BA.1 RBD-specific Ab titer was also significantly elevated after boosting with the Beta RBD-TM (Figure 5E). This boost may be explained in part by the 3.6-fold higher molar dose of RBD that is provided by an equal mass of RBD-TM vaccine. In more recent experiments to test boosting with Omicron BA.1 variant vaccines we compared the RBD-TM vaccines as a function of mass equivalent or molar equivalent doses. As before, mice were administered doses of ancestral whole-spike mRNA vaccine (8 μg per dose in this experiment) on days 0 and 21. On day 56, whole-spike or RBD-TM Omicron BA.1 vaccines were tested according to the booster protocol shown in Figure 5B. Group C mice received the equivalent mass of 8 μg RBD-TM, group D received 2 μg RBD-TM (90% of the equivalent molar dose of RBD). To investigate whether the reduced burden of LNP administered to group D could affect the immune response, we administered an additional 6 μg irrelevant mRNA (encoding nanoluciferase), formulated in the same manner, to group E. The data from this experiment as assessed by sVNT is shown in Figures 5F–5K. The multiplex sVNT assay provides a rich set of data allowing comparison of neutralization titers across a range of variant RBDs. Figures 5F–5H show that enhanced immunity induced by Omicron BA.1 RBD-TM mRNA is not dependent on higher molar dose of RBD. The 2-μg dose of RBD-TM was at least as effective as the 8-μg dose, both of which produced elevated $sVNT_{50}$ titers across the spectrum of variant RBDs.

In Figures 5I–5K the data are arranged to allow direct comparison of the booster vaccines against specific RBDs, i.e., ancestral, Omicron BA.1, and the recently widespread variant, XBB.1.5. Figure 5I shows that ancestral whole-spike boost is more effective at neutralizing ancestral spike than the whole-spike BA.1 vaccine. The RBD-TM vaccines were consistently more effective, although in groups of five mice, the differences were not statistically different. The data suggests that the BA.1 RBD-TM vaccine is equally effective at 8 or 2 μg with or without the 6-μg LNP-encapsulated nanoluciferase mRNA.

A similar heterologous boost experiment was carried out to evaluate BA.5 vaccines using doses of 5 μg mRNA in all cases. The protocol for the experiment is shown in Figure 6A. Mice received two doses of ancestral whole spike on days 0 and 21, followed by boosts with either ancestral whole spike, BA.5 whole spike, or BA.5 RBD-TM on day 56. Mice were euthanized on day 70 for analysis of serum using the multiplex sVNT assay. Figures 6B–6D show $sVNT_{50}$ values across the spectrum of variant RBDs. Boosting with ancestral whole spike provided better neutralization of early SARS-CoV-2 variants than the BA.5 whole-spike vaccine, but the BA.5 RBD-TM vaccine provided higher $sVNT_{50}$ titers across all variants, and was considerably more effective at neutralizing Omicron variants (shown in orange). Figures 6E and 6F show the data plotted as $sVNT_{50}$ titers provided by each vaccine against specific RBD variants. Figure 6E in accordance with Figure 5I demonstrates that boosting with a whole-spike Omicron variant reduces neutralizing capacity against the ancestral RBD.

Figures 6F and 6G show that boosting with BA.5 RBD-TM is more effective at neutralizing BA.5 or XBB.1.5 RBD binding to ACE2 than either whole-spike vaccine. Geometric mean $sVNT_{50}$ values obtained with BA.5 RBD-coated beads (Figure 6F) were 307, 644, and 11,203 ($n = 5$) for serum from mice vaccinated with ancestral whole spike, BA.5 whole spike, or BA.5 RBD-TM, respectively. The fold enhancement of geometric mean over ancestral whole spike was 2.1 for BA.5 whole spike and 36.4 for BA.5 RBD-TM. With groups of five animals (Figure 6F), the mean $sVNT_{50}$ values for BA.5 RBD binding were statistically different between ancestral spike and RBD-TM ($p = 0.011$), but not between BA.5 whole spike and RBD-TM whole spike ($p = 0.085$). Similar results were obtained for inhibition of binding of XBB.1.5 RBD to ACE2 (Figure 6G), with significant difference between BA.5 RBD-TM and ancestral whole spike ($p = 0.009$) but not between BA.5 RBD-TM and BA.5 whole spike ($p = 0.059$). The fold enhancement in geometric mean $sVNT_{50}$ over ancestral whole spike was 1.7 for BA.5 whole-spike vaccine and 25 for BA.5 RBD-TM vaccine, indicating the enhanced potential of the RBD-TM platform to overcome imprinting and effectively neutralize escape variants such as XBB.1.5.

To strengthen the significance of our heterologous boost studies, we carried out an analogous experiment on the performance of RBD-TM and whole-spike XBB.1.5 vaccines, using groups of eight mice, using both sVNT assays and authentic XBB.1.5 VNT assays (Figure 7). The format of the experiment was analogous to our previous BA.5 vaccine study (Figure 7A). sVNT assays indicated that the RBD-TM XBB.1.5 vaccine produced antibodies that were highly effective in inhibiting binding of Omicron RBD variants to ACE2, in particular BA.5, XBB, and the target XBB.1.5. Geometric mean $sVNT_{50}$ values

comparisons test, $^{*}p < 0.05$, $^{**}p < 0.01$. (F–H) Half-maximal inhibitory dilution $sVNT_{50}$ values determined in a multiplex RBD bead assay indicating the relative neutralization of binding of variant RBDs to ACE2 by mouse serum sampled on day 90, following day 56 boost with either 8 μg WT whole-spike (F), 8 μg Omicron BA.1 RBD-TM (G) or 2 μg Omicron BA.1 RBD-TM (H). $sVNT_{50}$s for early variants, Omicron variants, or SARS-CoV-1 are shown in green, orange, or blue, respectively. (I–K) Relative immunogenicity of five alternative boost vaccines administered on day 56, compared by determining $sVNT_{50}$ of day 90 mouse serum samples against WT SARS-CoV-2 RBD (I), Omicron BA.1 RBD (J), and Omicron XBB.1.5 RBD (K). Horizontal bars show the geometric mean; error bars show the geometric SD (in F–K) ($n = 5$ mice). For all panels, unless shown, multiple comparisons were not statistically significant.

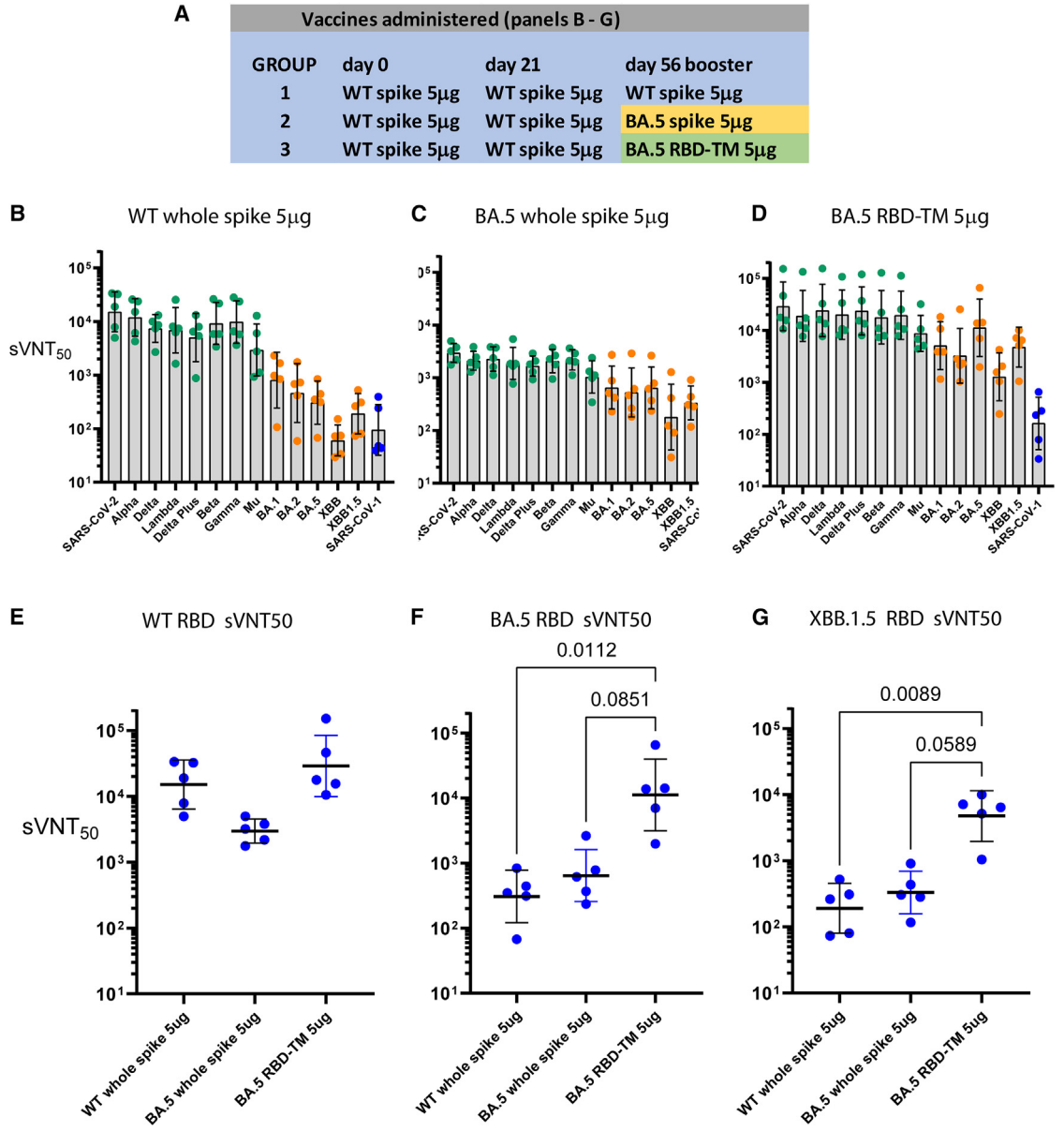

Figure 6. Heterologous boost study with Omicron BA.5 RBD-TM vaccine after exposure to WT whole-spike mRNA vaccine

(A) Vaccines administered to each group of mice in the heterologous boost study. (B–D) Half-maximal inhibitory dilution $sVNT_{50}$ values determined in a multiplex RBD bead assay indicating the relative neutralization of binding of variant RBDs to ACE2 by mouse serum sampled on day 90, following day 56 boost with either 5 µg WT whole-spike (B), 5 µg Omicron BA.5 whole-spike (C), or 5 µg Omicron BA.5 RBD-TM (D). (E–G) Relative immunogenicity of three alternative boost vaccines administered on day 56, compared by determining $sVNT_{50}$ of day 90 mouse serum samples against WT SARS-CoV-2 RBD (E), Omicron BA.5 RBD (F), and Omicron XBB.1.5 RBD (G). Horizontal lines or bars show the geometric mean; error bars show the geometric SD (in B–G) (n = 5 mice). Statistical analysis Kruskal-Wallis test with Dunn's multiple comparisons test. There were no significant differences in (E–G). The p values for multiple comparisons are shown in (F and G).

determined for serum induced by the RBD-TM vaccine were 11, 14, 12, and 12 times higher against BA.5, XBB, XBB.1.5, and JN.1 RBDs, respectively, than equivalent values for the whole-spike XBB.1.5 vaccine. The sVNT values for the three vaccines against either the ancestral RBD or the XBB.1.5 RBD are shown in Figures 7E and 7F. The RBD-TM XBB.1.5 vaccine matched the performance of the ancestral whole-spike vaccine against the ancestral RBD (Figure 7E). When performance against the XBB.1.5 RBD was analyzed, the sVNT data indicated that serum induced by the RBD-TM vaccine was significantly more effective at inhibiting binding of the XBB.1.5 RBD to ACE2, with a fold enhancement of geometric mean $sVNT_{50}$ of 16.3, compared with 1.3 for the whole-spike XBB.1.5 vaccine. Figure 7G

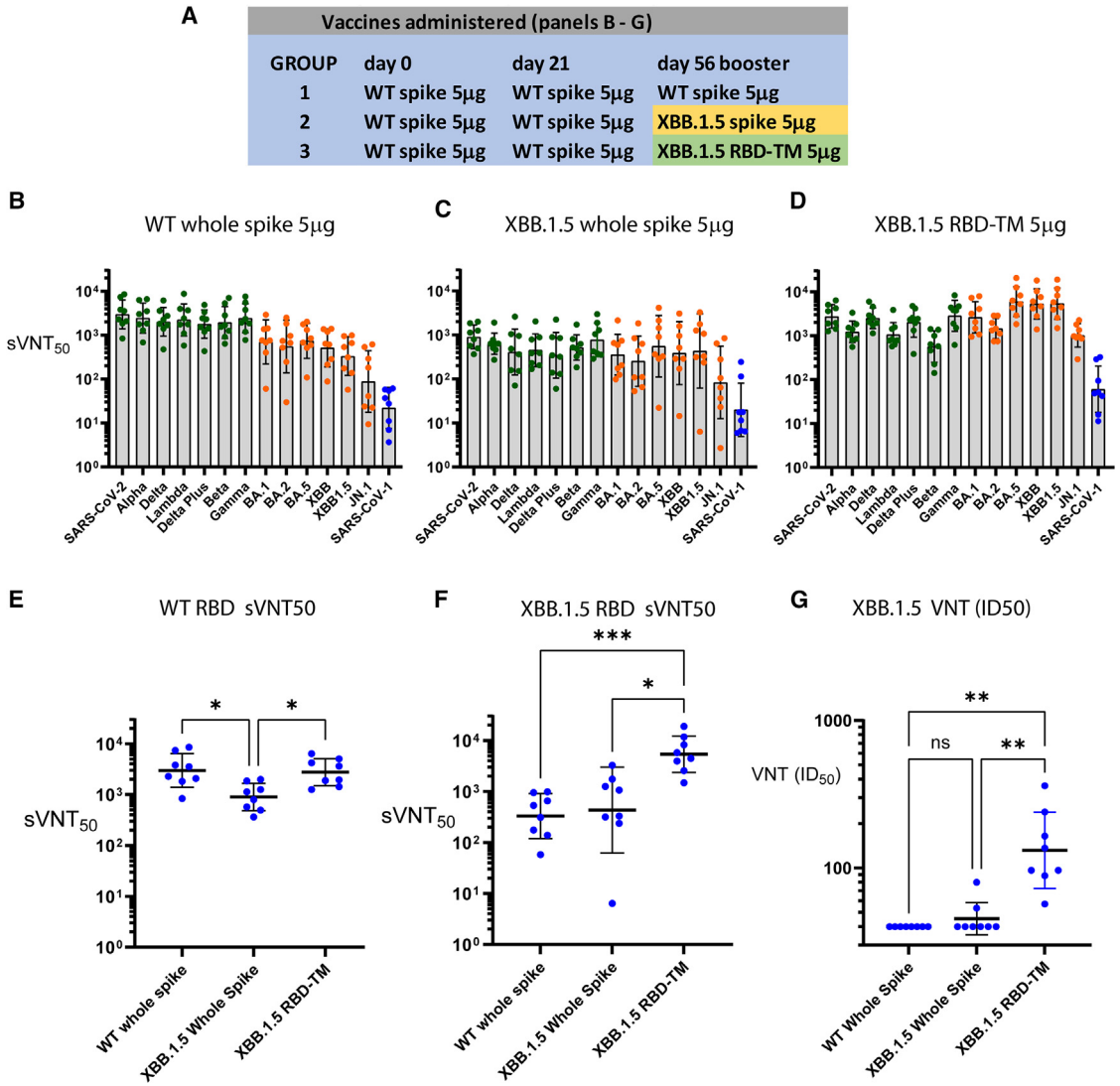

Figure 7. Heterologous boost study with Omicron XBB.1.5 RBD-TM vaccine after exposure to WT whole-spike mRNA vaccine

(A) Vaccines administered to each group of mice in the heterologous boost study. (B–D) Half-maximal inhibitory dilution $sVNT_{50}$ values determined in a multiplex RBD bead assay indicating the relative neutralization of binding of variant RBDs to ACE2 by mouse serum sampled on day 90, following day 56 boost with either 5 µg WT whole-spike (B), 5 µg Omicron XBB.1.5 whole-spike (C), or 5 µg Omicron XBB.1.5 RBD-TM (D). (E and F) Relative immunogenicity of three alternative boost vaccines administered on day 56, compared by determining $sVNT_{50}$ of day 90 mouse serum samples against WT SARS-CoV-2 RBD (E) or Omicron XBB.1.5 RBD (F). (G) Neutralization of XBB.1.5 virus infection of Vero cells by serum samples collected on day 90. Where neutralization was not detected, the individual samples are at the limit of detection of 40. In (B–G), the horizontal lines or bars show geometric mean; error bars show geometric SD (n = 8 mice). Statistical analysis Kruskal-Wallis test with Dunn's multiple comparisons test $^{*}p < 0.05$, $^{**}p < 0.01$, $^{***}p < 0.001$.

shows the ability of serum samples to neutralize infection of Vero cells by the XBB.1.5 virus. This assay requires larger volumes of serum that, in practice, were achieved by diluting the serum at least 40 times. When neutralization was not detected at a dilution of 1 in 40, the serum sample is plotted at the limit of detection of 40, and was attributed a VNT (ID_{50}) of 40, although in many cases VNT (ID_{50}) would have been considerably lower if larger volumes of serum were available. After XBB.1.5 whole-spike vaccine, only two of eight serum samples had VNT (ID_{50}) values above 40. Non-parametric analysis indicated that serum samples from mice vaccinated with XBB.1.5 RBD-TM was significantly more effective ($p < 0.01$) in neutralizing the XBB.1.5 virus than serum from mice vaccinated with either ancestral or XBB.1.5 whole-spike vaccines.

DISCUSSION

Vaccination with the ancestral whole-spike of SARS-CoV-2, and/or infection with one or more variants of the ancestral virus, have induced a level of immunity in most individuals that allows them

to overcome infection by current variants of Omicron without suffering serious illness.[3–5,7] In contrast, during the early stages of the pandemic in 2020 and 2021, many individuals required hospitalization. The whole-spike vaccines, combined with use of face masks and the introduction of social distancing strategies, were effective in preventing hospital systems from becoming overwhelmed with patients requiring intensive care, or at least close monitoring. In late 2024, close to 4 years after the onset of the COVID-19 pandemic, the mortality rate was considerably lower than it was during the first 2 years, but there are still many deaths occurring that are associated with COVID infection.[26]

To reduce the incidence of COVID-related deaths, there is a need for broad-spectrum second-generation vaccines that can protect elderly and vulnerable individuals from infection by emerging variants of SARS-CoV-2 or other known betacoronaviruses. Whole-spike mRNA booster vaccines have been modified over the past 2 years to include mutations found in the RBD of Omicron variants BA.4/5 and XBB.1.5. Initially, the updated vaccines were introduced as bivalent products including the ancestral spike.[8] The bivalent vaccines are more effective as boosters against Omicron than the ancestral spike alone,[7] but the phenomenon of immune imprinting seems to limit the ability of variant whole-spike vaccines to induce high titers of new neutralizing antibodies against the emerging Omicron variants.[5,6,14,16,27] The most recently updated whole-spike vaccines, which may offer more protection, target the XBB.1.5 variant, as recommended by the World Health Organization[28]; however, other variants such as EG.5 and recent mutants derived from BA.2.86 (e.g., JN.1) are currently increasing in prevalence.

The RBD-TM mRNA vaccine platform offers the opportunity to develop multivalent vaccines that can be adapted to combine relevant circulating variant SARS-CoV-2 RBDs to prevent infection as the virus mutates. The RBD-TM vaccine has several advantages. Most important, as demonstrated in Figures 5, 6, and 7, boosting with RBD-TM mRNAs, after two doses of ancestral whole-spike vaccine, results in induction of new variant-specific antibodies, 20–50 times more effective in preventing binding of target RBDs to ACE2. Second, as demonstrated by Figures 1G–1K and S5, on a mass basis the RBD-TM mRNA is more potent that its whole-spike equivalent. The two vaccine platforms are equipotent on a molar basis. This implies that it will be possible to administer tri- or tetra-valent RBD-TM vaccines without exceeding the 30- to 50-μg doses of formulated mRNA that are currently in use. The reactogenicity of mRNA-LNP formulations is likely to limit any increase in total dose of mRNA beyond the current dose levels. Data from our phase 1 clinical study supported the potential of the RBD-TM platform by confirming that 10 μg RBD-TM mRNA provides an effective booster dose in humans.[21] Third, in the setting of a real-world heterologous boost (Figures 5, 6, and 7), the RBD-TM induces antiserum which offers some protection against later RBD variants. For example, vaccination with 5 μg BA.5 RBD-TM mRNA induced antisera with geometric mean $sVNT_{50}$ values greater than 1,000 against the more recent Omicron variants, XBB (1279) and XBB.1.5 (4770) (Figure 6D), fold enhancements of 7 and 14 over the equivalent geometric mean sVNT values (179 and 332) associated with the whole-spike BA.5 vaccine. Subsequent experiments to test the value of heterologous booster vaccines targeted against XBB.1.5 (Figure 7), using larger groups of mice, provided a clear demonstration, suing both sVNT and authentic VNT assays, that the RBD-TM XBB.1.5 vaccine significantly outperformed the whole-spike equivalent vaccine.

Experiments using the Beta RBD-TM vaccine indicated that $VNT(ID_{50})$ values greater than 200–300 (Figure 3E) were adequate to achieve full protection when the same mice were challenged with live virus (Figures 3F and 3G). These data suggest that multivalent RBD-TM vaccines have the potential to protect against future escape variants. The design of multivalent vaccines is likely to improve when more data is available to help predict which RBD-TM variant vaccines have broad spectrum activity, as exemplified by the unexpected activity of the Kappa RBD-TM vaccine (Figures 4A and S10).

The precise mechanisms of action of the RBD-TM and whole-spike vaccines remain to be elucidated. We hypothesized that the presentation of the whole-spike protein at the surface of cells might be an important determinant of the success of the approved mRNA vaccines. Hence, we decided to include the TM domain and CT of the spike protein so that the translated protein would be expressed in an analogous manner as a membrane-anchored protein. We do not anticipate that RBD-TM trimers are formed, although we cannot rule out the possibility.

The tissues and cell types where protein translation occurs are critical to the induction of the immune response to whole-spike mRNA. It is known that muscle tissue translates the most protein after IM injection of mRNA formulated in LNPs, but the most important events may occur when LNPs interact with immune cells during their drainage to lymph nodes. This hypothesis is supported by our published work in which we studied the effect of LNP formulation and were able to correlate the translation of nanoluciferase reporter mRNA in lymphoid tissues with induction of immunity after IM injection of mRNA encoding ovalbumin.[29]

We know from unpublished work that phagocytic cells (macrophages and dendritic cells) take up LNPs and translate mRNA,[30] but how this results in presentation to B cells or T cells is not known. We posit that, whichever cells are involved, the translation of RBD-TM mRNA occurs at the surface of the endoplasmic reticulum and the secretion signal sequence subsequently results in presentation of a plasma membrane-anchored RBD. We concluded early in our studies (Figures 1G–1K) that, perhaps surprisingly, presentation of the RBD-TM in this way is equivalent, with respect to the molarity of RBD moieties, to presentation of RBD as a component of the trimeric whole-spike protein. This implies that the location of the RBD translated from RBD-TM mRNA and its subsequent processing by antigen-presenting cells is likely to be similar to the presentation of RBD antigens from whole-spike mRNA.

The LNP formulation used for the preclinical studies described here, and also for our phase 1 clinical study,[21] made use of lipids that have been previously used in US Food and Drug Administration-approved products for human use. The ionizable lipid, DLin-MC3-DMA, is used in Onpattro,[31] as are DSPC and cholesterol. The latter two structural or helper lipids are also used in the Moderna mRNA vaccine, Spikevax, as is the neutral PEGylated lipid, DMG-PEG_{2000}, which we used throughout this study.[32]

We used an LNP formulation with some differences to the 'standard' Onpattro formula, which uses ionizable lipid, cholesterol, DSPC and the PEGylated lipid, PEG_{2000}-C-DMG, in the following ratio; 50:38.5:10:1.5 mol%.[31] First, we typically used a formula with reduced PEGylated lipid content, i.e., 50:39.85:10:0.15 mol%. Second, we reduced the total lipid content, usually characterized by an N/P ratio of 6, to an N/P ratio of 5, where N/P ratio denotes the molar ratio of DLin-MC3-DMA to nucleotide, i.e., the molar ratio of ionizable nitrogen atoms to anionic phosphate moieties. These changes have the effect of producing LNPs that are typically larger (in the 120- to 160-nm range as compared with the 60- to 100-nm range) and which are more negatively charged (−5 to −10 mv) than standard LNPs (0 to −5 mv). By considering the available surface area and availability of PEGylated lipids, we estimate that, before administration, our LNPs have a reduced mantle of PEG at the LNP-water interface, which may affect uptake by phagocytic cells. However, we recognize that the surface properties of DMG-PEG_{2000}-coated LNPs will be substantially changed, by interaction with lipoproteins and plasma proteins, when they reach the blood circulation after intramuscular injection.[33]

The modifications in lipid molar ratios we made to the standard LNP formula were based on our previous, as yet unpublished, observations.[30,34] Before our work on the COVID vaccine we were investigating the effect of size, charge and PEGylated lipid content on biodistribution. We found that after intravenous injection, larger, more negatively charged particles are extracted to a lesser extent by the mouse liver. This results in a higher mass ratio of mRNA translation in spleen versus liver.[30,34] We posit that this redistribution, and reduction in liver uptake, is desirable for vaccination, in contrast with the aim of the Onpattro product, which was designed for the delivery of small interfering RNA to the liver.[31]

The spleen/liver redistribution is evident when the PEGylated lipid content is reduced within the range 0.15–0.25 mol% PEGylated lipid and with an N/P ratio of 5.[30,34] We found that redistribution correlated with improved translation of reporter mRNA in phagocytic cells in the spleen and improved cell-mediated responses to vaccination of mice with mRNA encoding ovalbumin. The redistribution correlates with the observation by Siegwart and colleagues,[35–37] who also showed that negative charge is associated with delivery to the spleen.

ELISAs and VNT assays using serum from vaccinated naive mice suggested that immunity against the target antigen was predictable, reproducible, and approximated to a linear function of dose of mRNA over the range 0.3 to 3 μg. Ab titers and VNT(ID_{50}) titers were only marginally higher at the 10-μg doses against the target variant, but the improvement in broad-spectrum activity at higher doses was evident from the multiplex sVNT assays. This implies that the design of multivalent RBD-TM vaccines will require careful analysis of the breadth of activity produced by specific mRNAs. The surprising strength and breadth of activity of the Kappa RBD-TM vaccine illustrates this point. Analysis of the data from multiplex sVNT assays[38] suggested that this is a precise and reliable approach for analyzing breadth of immune responses. The rank order of $sVNT_{50}$ values was consistent with our expectations, based on the degree of similarity between target variant vaccine and each alternative RBD tested. When we were able to compare sVNT data with neutralization studies using viral infection of Vero cells, there was good agreement between the two assay methods. This supports data suggesting that neutralizing antibodies are predominantly bound to the RBD.[36] Consequently, we suggest that sVNT assays using serum from vaccinated mice will provide accurate predictions of protection induced by specific RBD-TM vaccines against emerging or pre-emergent RBD variants.

Since the onset of the COVID pandemic, there has been interest in the potential of RBD-based vaccines, given the proportion of neutralizing antibodies that bind to the RBD.[39] The majority of RBD vaccine candidates in clinical development are recombinant proteins, though there have been two notable mRNA candidates. A mRNA vaccine encoding secreted $RBD^{(319–541)}$, ARCoV-mRNA, was developed in China by Walvax/Abogen and is now approved for use in Indonesia.[40] Early in BioNTech/Pfizer's clinical program, a secreted RBD fusion protein modified with the addition of a T4 fibritin-derived foldon domain, designed to form a trimeric complex (BNT162b1), was tested in a phase 1 study.[41] This candidate did not progress when the whole-spike vaccine BNT162b2 was selected for its phase 3 efficacy study.[2] The RBD-TM platform described here has been evaluated in a joint phase 1 clinical trial using the Beta variant RBD-TM in parallel with an adjuvanted Beta RBD-Fc protein vaccine.[21,23] Given that the ancestral vaccines offered comparatively good neutralization of the Beta variant, as compared with Omicron variants, it was not clear how well the RBD-TM vaccine was able to overcome immune imprinting in humans. A subsequent clinical efficacy study using a contemporary Omicron variant would be valuable.

How the membrane-anchored RBD-TM compares with secreted RBD vaccines in terms of mechanism of action and potency is not known but is currently under investigation. We were not aware of any other parallel developments of membrane-anchored mRNA RBD vaccines until a recent report of a phase 1 clinical study of a self-amplifying RNA construct was published.[42] The advantage of mRNA RBD-based vaccines is the speed with which the product can be modified as the virus mutates, and the potential for design of multivalent vaccines. The shorter RBD-TM design will allow multivalent vaccines to be produced without risking increased reactogenicity. The challenge will be to outflank the RBD mutation of the virus by anticipating the emergence of evasive mutants,[17,43–45] making use of the developing knowledge of likely hot spots in the RBD, and deep

scans that identify which mutations are tolerated without loss of ACE2 binding.[46–48]

MATERIALS AND METHODS

Study design

The objectives of the study were to determine whether (1) RBD-TM mRNA SARS-CoV-2 vaccines were as effective as whole-spike vaccines in mice; (2) RBD-TM vaccines could be tailored to vaccinate against alternative variants of SARS-CoV-2 and produce broad spectrum vaccines; and, most important, (3) RBD-TM vaccines are able to induce new Ab production against new variants against a background of immune imprinting with ancestral whole-spike protein. The preclinical studies also allowed us determine a suitable range of doses for a clinical study of an RBD-TM vaccine, which was carried out in parallel with ongoing preclinical experiments. We used mice for the majority of the preclinical studies, but also carried out some challenge tests in Syrian hamsters and a vaccine toxicity study in rats. For comparison of immune responses to vaccines, i.e., dose response studies, comparisons between RBD-TM and whole-spike vaccines, or comparisons between formulations, the experiments were usually carried out using groups of five mice for each treatment. This number of mice per group was generally adequate to compare the effectiveness of RBD-TM and whole-spike vaccines and served to keep animal numbers within acceptable limits as approved by Monash Institute of Pharmaceutical Sciences animal ethics committee. To increase statistical power, we used eight mice per group in an evaluation of XBB.1.5 vaccines, which provided more convincing statistical significance. Data were not excluded under any circumstances. To avoid investigator bias, serum samples from mice were coded so that the laboratory scientists carrying out ELISA and neutralization tests were unaware of which serum samples were under analysis. Biological variation of immune responses within groups of animals was generally greater than between experiments comparing replicate batches of vaccine formulations. Routine replicates using different batches were not carried out.

RBD-TM mRNA production

The mRNAs used in this study were produced using HiScribe T7 mRNA synthesis kit (NEB) using linearized DNA produced by PCR amplification. The transcribed mRNAs included a 3′-UTR with Kozak sequence and 5′-UTR, both designed *de novo*, and included polyA$_{125}$ tails. The sequences were optimized to reduce the uridine content of mRNA. We used N1-methyl-pseudoUTP instead of UTP to produce chemically modified mRNA, in common with the two approved COVID-19 vaccines.[19] CleanCap reagent AG (TriLink) was used in accordance with the manufacturer's recommendations to produce Cap1 chemistry at the 5′ terminus. The mRNA was subject to cellulose purification before use.[49] The design of RBD-TM mRNA is exemplified by the ancestral RBD-TM mRNA sequence shown in Figure S1. To compare the RBD-TM with whole-spike vaccines, we introduced the BioNTech/Pfizer whole-spike coding sequence (which we obtained from whom International Nonproprietary Names document 11889 in September 2020) in place of the RBD-TM, i.e., we used the same UTRs and polyA tail for RBD-TM and whole-spike vaccines.

LNP formulation

The following lipids were used in the study: the ionizable lipids used for most studies was (6*Z*,9*Z*,28*Z*,31*Z*)-heptatriaconta-6,9,28,31-tetraen-19-yl-4-(dimethylamino)butanoate ('DLin-MC3-DMA', MedChem Express) and for comparisons we used [(4-hydroxybutyl)-azanediyl]-di-(hexane-6,1-diyl)-bis-(2-hexyldecanoate) (ALC-0315). The commonly used helper lipids were cholesterol (Sigma-Aldrich) and DSPC (Avanti Polar Lipids Inc.). The PEGylated lipid used was 1,2-dimyristoyl-rac-glycero-3-methoxypolyethylene glycol-2000 (DMG-PEG 2000) (Avanti Polar Lipids Inc.). Formulations of the vaccines into LNPs involved the following steps: an aqueous solution of mRNA at pH 4 was mixed with a solution of the four lipids in ethanol, using a microfluidics mixing device (NxGen Ignite Nanoassemblr) supplied by Precision Nanosystems. The suspension of nanoparticles was adjusted to a pH of 7.4 using a 1:3 dilution in Tris buffer, then dialyzed against 25 mM Tris buffer to remove the ethanol. The LNP suspension was adjusted with sucrose solution (8.8% w/v) to produce the cryoprotected, isotonic final form of the product. The product was sterile filtered (0.22 μm) before being aliquoted into sterile vials for storage at −80°C. Characterization of the LNPs included analysis for RNA content, encapsulation efficiency, RNA integrity. Particle size and polydispersity index (PDI) were determined by dynamic light scattering, a standard method for submicron dispersions, using a Zetasizer (Malvern Instruments). Typically, encapsulation efficiency was 85%–95%, particle size (Z-average) of the 0.15% PEGylated lipid formulation was 120–160 nm with a PDI of <0.2. The particle sizes of 0.15% PEG-DMG LNPs were larger than the typical sizes of 80–100 nm for standard LNPs. Apparent Zeta potentials were slightly negative but close to neutral (−5 to −10 mv) and, therefore, difficult to determine precisely. After thawing, there were no changes in zeta potential but the apparent particle size of both 0.15% and 1.5% PEG-DMG LNPs increases, typically by 10–20 nm. We have not carried out an industry-standard physical stability analysis on the LNPs before storage, but we have assessed stability of the 0.15% DMG-PEG particles and found no changes in particle size over 1 month at 2–8°C.

Intramuscular inoculation of mice

All animal experiment procedures described were conducted under the approval of the Monash Institution of Pharmaceutical Science Animal Ethics Committee (Refs 2020-23982-42711 and 2023-40140-97716). BALB/c mice were vaccinated by injection of LNP-mRNA suspension (50 μL) into the calf muscle. In early studies female BALB/c mice were used aged between 8 and 12 weeks old at the start of the study. Mice were primed on day 0 and boosted on day 21. Mice were bled just before the second injection, and typically 3 weeks (day 42) and 5 weeks (day 56) following the second injection. Viral challenge studies were carried out on day 65. For heterologous boost experiments, BALB/c mice (n = 5 per group) were vaccinated on days 0 and 21 with a mRNA-LNP vaccine produced in house encoding the whole spike of ancestral SARS-CoV-2. On day 56, the mice were vaccinated for

the third time with one of a series of test booster vaccines. Mice were bled on days 21, 56, and at later times after the booster vaccine. In later heterologous boost studies (Figure 7), we used equal numbers of male and female BALB/c mice (four males and four females in each group of eight mice). No differences in immune responses were observed between male and female mice.

ELISA for measurement of RBD-specific Ab responses

Wild-type (WT) and variant RBD-specific total Ab responses in the sera of mice before and after inoculation were investigated by ELISA using the RBD monomer from either the WT, Beta, or Omicron BA.1 variant strain. Flat-bottom 96-well maxisorp plates (Thermo Fisher Scientific) were coated with 50 μL/well of RBD monomer at a concentration of 2 μg/mL in Dulbecco's PBS (Gibco Life Technologies). Plates were incubated overnight at 4°C, after which unbound RBD monomer was removed, and wells were blocked with 100 μL/well of 1% bovine serum albumin (BSA fraction V, Invitrogen Corporation, Gibco) in PBS for 1–2 h before washing with PBS containing 0.05% v/v Tween 20. Mouse sera were added to wells and left to incubate overnight at room temperature. After washing, bound Ab was detected using horseradish peroxidase-conjugated rabbit anti-mouse Ig Abs (Dako). The detection Ab was incubated for 1 h at room temperature in a humidified atmosphere and the plates then washed five times with PBS/0.1% Tween 20. Wes added 100 μL tetramethylbenzidine substrate (TMB, BD Biosciences) to each well for 5–7 min before the reaction was stopped using 100 μL/well of 1 M orthophosphoric acid (BDH Chemicals). The optical density (OD) of each well was determined at wavelengths of 450 nm and 540 nm. Titers of Ab were expressed as the reciprocal of the highest dilution of serum required to achieve an OD of 0.3, which represents at least five times the background level of binding.

In vitro microneutralization assay (VNT)

SARS-CoV-2 isolates hCoV/Australia/VIC01/2020 (Ancestral) and hCoV/Australia/QLD1520/2020 (Beta) were passaged in Vero cells and aliquots stored at −80°C. Mouse serum samples were heat inactivated at 56°C for 45 min before use. Serum was serially diluted in MEM medium, followed by the addition of 100 50% tissue culture ID ($TCID_{50}$) of SARS-CoV-2 in MEM/0.5% BSA and incubation at room temperature for 45 min. Vero cells were washed twice with serum-free MEM before the addition of MEM containing 1 μg/mL of TPCK trypsin. Vero cells were then inoculated in quadruplicate with the plasma:virus mixture and incubated at 37°C and 5% CO2 for 3–5 days. For SARS-CoV-2 omicron variants hCoV-19/Australia/NSW/RPAH-1933/2021 [BA.1], hCoV-19/Australia/VIC/35864/2022 [BA.2] and hCoV-19/Australia/VIC/55437/2022 [BA.4], variants were passaged in Calu3 cells in DMEM with 2% FCS and microneutralization assays were performed in Vero E6-TMPRSS2 cells. The cytopathic effect was scored, and the neutralizing Ab titer was calculated using the Reed–Muench method.

RBD-ACE2 multiplex inhibition assay

For multiplex determination of surrogate VNT titers (sVNTs), we adapted the Luminex platform as described previously.[38] AviTag-biotinylated RBD proteins from different SARS-CoV-2 variants and other sarbecoviruses were coated on MagPlex-Avidin microspheres (Luminex) at 5 μg per 1 million beads. RBD-coated microspheres (600 beads per antigen) were preincubated with serum at a final dilution of 1:20 or greater for 1 h at 37°C with 800 rpm agitation. After 1 h of incubation, 50 μL of phycoerythrin-conjugated human ACE2 (1 μg/mL; GenScript) was added to the well and incubated for 30 min at 37°C with agitation, followed by two washes with 1% bovine serum albumin in PBS. The final readings were acquired using a MAGPIX reader (Luminex) and expressed as half-maximal inhibitory dilution ($sVNT_{50}$).

Mouse SARS-CoV-2 challenge model

Protective efficacy against upper (nasal turbinates) and lower (lung) airways infection was assessed using a mouse SARS-CoV-2 challenge model with a human clinical isolate of SARS-CoV-2, VIC2089 (N501Y) variant (hCoV-19/Australia/VIC2089/2020) or a naturally arising Beta (K417N, E484K, N501Y) variant, B.1.351. Vaccinated and unvaccinated control mice were aerosol challenged with 1.5×10^7 $TCID_{50}$ infectious units of VIC2089 or B.1.351 using either an inhalation exposure system (Glas-col) (Figure 1) or venturi nebulization (Figure 3). Three days later, challenged mice were euthanized and infectious virus titers ($TCID_{50}$) in the lungs (Figures 1 and 3) and nasal turbinates (Figure 3) of individual mice were determined by serial dilution of lung or nasal supernatants onto confluent Vero cell (clone CCL81) monolayers. Plates were incubated at 37°C for 4 or 5 days before measuring cytopathic effect under an inverted phase contrast microscope. $TCID_{50}$ was calculated using the Spearman and Krber method.

Statistical methods

Non-parametric ANOVA using the Kruskal-Wallis test was used throughout. Dunn's multiple comparisons test was used to compare differences between treatment groups. All statistical analysis was carried out using GraphPad Prism (version 10.1.2).

DATA AND CODE AVAILABILITY

All data are available in the main text or the supplemental information.

ACKNOWLEDGMENTS

This work was supported primarily by grants from the Australian Medical Research Future Fund (MRFF), the Victorian State Government entity, mRNA Victoria. G.D. was supported by philanthropic funds from IFM, D.I.G. was supported by an NHMRC Investigator Award 2008913. The following colleagues are acknowledged for their support or comments during the study: Mason Littlejohn, Jason Mackenzie, Joseph Torresi, Stephen Kent, Adam Wheatley, Sharon Lewin, David Jackson, and Kanta Subbarao. Drew Brockman and Peter Tapley (Agilex Biolabs) are acknowledged for their participation in the rat toxicity studies reported in the supplementary materials. Thanks to Julian Druce and Leon Caly (Victorian Infectious Disease Reference Laboratory) for isolating and distributing ancestral and variant SARS-CoV-2 virus during the course of this study. Funding: Medical Research Future Fund (MRFF) Award 2005846: D.I.G., T.M.N., D.F.J.P., G.D., S.R., and C.W.P.; Victorian Government, mRNA Victoria: D.F.J.P. and C.W.P.; Monash University PhD Scholarships: T.P., A.T., and H.S.; Australian National Health and Medical Research Council 2008913: D.I.G.; Singapore National Medical Research Council (MOH-COVID19 RF-003); IFM investors: G.D.

AUTHOR CONTRIBUTIONS

Conceptualization: C.W.P. and H.A.W.; Methodology: H.A.W., S.A.F., C.W.T., J.M., P.E., K.C.D., R.B., and G.D.; Investigation: H.A.W., S.L.G., R.K., J.K.H., S.L.Y.T., C.W.T., T.J.P., A.T., H.S., J.M., P.E., J.P.C., K.C.D., and G.D.; Visualization: C.W.P., M.P., S.R., D.I.G., T.M.N., L.-F.W., and D.F.J.P.; Funding acquisition: C.W.P., D.I.G., D.F.J.P., and T.M.N.; Project administration: C.W.P. and D.I.G.; Supervision: C.W.P., R.B., M.P., L.-F.W., D.F.J.P., and G.D.; Writing – original draft: C.W.P.; Writing – review & editing: All authors.

DECLARATION OF INTERESTS

Two provisional patents (PCT/AU2022/050912 and PCT/AU2022/050913) covering the RBD-TM mRNA vaccine design and the LNP formulation used in this study, and underlying technology, have been submitted through Monash University, with C.W.P., H.A.W., and S.A.F. as co-inventors of 050912 and C.W.P., H.A.W., and J.K.H. as co-inventors of 050913. C.W.T. and L.-F.W. are co-inventors of a patent on the surrogate VNT test (sVNT) platform. T.N. receives research contracts to conduct clinical trials, with funding to institutions from Moderna, SanofiPasteur, GSK, Iliad Biotechnologies, Dynavax, Seqirus, Janssen, and MSD. T.N. receives consulting fees from GSK, Seqirus, MSD, SanofiPasteur, AstraZeneca, Moderna, BioNet, and Pfizer. T.N. serves on DSMBs for Seqirus, Clover, Moderna, Emergent, Serum Institute of India, SK Bioscience Korea, Emergent Biosolutions, and Novavax. S.R. is an employee of CSL Seqirus that is a maker of influenza vaccines. C.Y.W. is a shareholder of Ena Respiratory. D.I.G. has received research funding from CSL for an unrelated project.

SUPPLEMENTAL INFORMATION

Supplemental information can be found online at https://doi.org/10.1016/j.omtm.2024.101380.

REFERENCES

1. Baden, L.R., El Sahly, H.M., Essink, B., Kotloff, K., Frey, S., Novak, R., Diemert, D., Spector, S.A., Rouphael, N., Creech, C.B., et al. (2021). Efficacy and Safety of the mRNA-1273 SARS-CoV-2 Vaccine. N. Engl. J. Med. *384*, 403–416.
2. Polack, F.P., Thomas, S.J., Kitchin, N., Absalon, J., Gurtman, A., Lockhart, S., Perez, J.L., Pérez Marc, G., Moreira, E.D., Zerbini, C., et al. (2020). Safety and Efficacy of the BNT162b2 mRNA Covid-19 Vaccine. N. Engl. J. Med. *383*, 2603–2615.
3. Bar-On, Y.M., Goldberg, Y., Mandel, M., Bodenheimer, O., Amir, O., Freedman, L., Alroy-Preis, S., Ash, N., Huppert, A., and Milo, R. (2022). Protection by a Fourth Dose of BNT162b2 against Omicron in Israel. N. Engl. J. Med. *386*, 1712–1720.
4. Grewal, R., Kitchen, S.A., Nguyen, L., Buchan, S.A., Wilson, S.E., Costa, A.P., and Kwong, J.C. (2022). Effectiveness of a fourth dose of covid-19 mRNA vaccine against the omicron variant among long term care residents in Ontario, Canada: test negative design study. BMJ *378*, e071502.
5. Regev-Yochay, G., Gonen, T., Gilboa, M., Mandelboim, M., Indenbaum, V., Amit, S., Meltzer, L., Asraf, K., Cohen, C., Fluss, R., et al. (2022). Efficacy of a Fourth Dose of Covid-19 mRNA Vaccine against Omicron. N. Engl. J. Med. *386*, 1377–1380.
6. Wang, Q., Guo, Y., Iketani, S., Nair, M.S., Li, Z., Mohri, H., Wang, M., Yu, J., Bowen, A.D., Chang, J.Y., et al. (2022). Antibody evasion by SARS-CoV-2 Omicron subvariants BA.2.12.1, BA.4 and BA.5. Nature *608*, 603–608.
7. Chalkias, S., Eder, F., Essink, B., Khetan, S., Nestorova, B., Feng, J., Chen, X., Chang, Y., Zhou, H., Montefiori, D., et al. (2022). Safety, immunogenicity and antibody persistence of a bivalent Beta-containing booster vaccine against COVID-19: a phase 2/3 trial. Nat. Med. *28*, 2388–2397.
8. Administration, USFD (2023). Coronavirus (COVID-19) Update: FDA Authorizes Moderna, Pfizer-BioNTech Bivalent COVID-19 Vaccines for Use as a Booster Dose. https://www.fda.gov/news-events/press-announcements/coronavirus-covid-19-update-fda-authorizes-moderna-pfizer-biontech-bivalent-covid-19-vaccines-use.
9. Lin, D.Y., Du, Y., Xu, Y., Paritala, S., Donahue, M., and Maloney, P. (2024). Durability of XBB.1.5 Vaccines against Omicron Subvariants. N. Engl. J. Med. *390*, 2124–2127.
10. Aydillo, T., Rombauts, A., Stadlbauer, D., Aslam, S., Abelenda-Alonso, G., Escalera, A., Amanat, F., Jiang, K., Krammer, F., Carratala, J., and García-Sastre, A. (2021). Immunological imprinting of the antibody response in COVID-19 patients. Nat. Commun. *12*, 3781.
11. Reynolds, C.J., Pade, C., Gibbons, J.M., Otter, A.D., Lin, K.M., Muñoz Sandoval, D., Pieper, F.P., Butler, D.K., Liu, S., Joy, G., et al. (2022). Immune boosting by B.1.1.529 (Omicron) depends on previous SARS-CoV-2 exposure. Science *377*, eabq1841.
12. Henry, C., Palm, A.K.E., Krammer, F., and Wilson, P.C. (2018). From Original Antigenic Sin to the Universal Influenza Virus Vaccine. Trends Immunol. *39*, 70–79.
13. Wheatley, A.K., Fox, A., Tan, H.X., Juno, J.A., Davenport, M.P., Subbarao, K., and Kent, S.J. (2021). Immune imprinting and SARS-CoV-2 vaccine design. Trends Immunol. *42*, 956–959.
14. Wang, Q., Bowen, A., Valdez, R., Gherasim, C., Gordon, A., Liu, L., and Ho, D.D. (2023). Antibody Response to Omicron BA.4-BA.5 Bivalent Booster. N. Engl. J. Med. *388*, 567–569.
15. Wang, Q., Guo, Y., Tam, A.R., Valdez, R., Gordon, A., Liu, L., and Ho, D.D. (2023). Deep immunological imprinting due to the ancestral spike in the current bivalent COVID-19 vaccine. Preprint at bioRxiv. https://doi.org/10.1101/2023.05.03.539268.
16. Wang, Q., Iketani, S., Li, Z., Liu, L., Guo, Y., Huang, Y., Bowen, A.D., Liu, M., Wang, M., Yu, J., et al. (2023). Alarming antibody evasion properties of rising SARS-CoV-2 BQ and XBB subvariants. Cell *186*, 279–286.e8.
17. Cao, Y., Jian, F., Wang, J., Yu, Y., Song, W., Yisimayi, A., Wang, J., An, R., Chen, X., Zhang, N., et al. (2023). Imprinted SARS-CoV-2 humoral immunity induces convergent Omicron RBD evolution. Nature *614*, 521–529.
18. Ma, W., Fu, H., Jian, F., Cao, Y., and Li, M. (2023). Immune evasion and ACE2 binding affinity contribute to SARS-CoV-2 evolution. Nat. Ecol. Evol. *7*, 1457–1466.
19. Xia, X. (2021). Detailed Dissection and Critical Evaluation of the Pfizer/BioNTech and Moderna mRNA Vaccines. Vaccines (Basel) *9*, 734.
20. Walsh, E.E., Frenck, R.W., Jr., Falsey, A.R., Kitchin, N., Absalon, J., Gurtman, A., Lockhart, S., Neuzil, K., Mulligan, M.J., Bailey, R., et al. (2020). Safety and Immunogenicity of Two RNA-Based Covid-19 Vaccine Candidates. N. Engl. J. Med. *383*, 2439–2450.
21. Nolan, T.M., Deliyannis, G., Griffith, M., Braat, S., Allen, L.F., Audsley, J., Chung, A.W., Ciula, M., Gherardin, N.A., Giles, M.L., et al. (2023). Interim results from a phase I randomized, placebo-controlled trial of novel SARS-CoV-2 beta variant receptor-binding domain recombinant protein and mRNA vaccines as a 4th dose booster. EBioMedicine *98*, 104878.
22. Zeng, B., Gao, L., Zhou, Q., Yu, K., and Sun, F. (2022). Effectiveness of COVID-19 vaccines against SARS-CoV-2 variants of concern: a systematic review and meta-analysis. BMC Med. *20*, 200.
23. Deliyannis, G., Gherardin, N.A., Wong, C.Y., Grimley, S.L., Cooney, J.P., Redmond, S.J., Ellenberg, P., Davidson, K.C., Mordant, F.L., Smith, T., et al. (2023). Broad immunity to SARS-CoV-2 variants of concern mediated by a SARS-CoV-2 receptor-binding domain protein vaccine. EBioMedicine *92*, 104574.
24. Zhang, B.Z., Wang, X., Yuan, S., Li, W., Dou, Y., Poon, V.K.M., Chan, C.C.S., Cai, J.P., Chik, K.K., Tang, K., et al. (2021). A novel linker-immunodominant site (LIS) vaccine targeting the SARS-CoV-2 spike protein protects against severe COVID-19 in Syrian hamsters. Emerg. Microbes Infect. *10*, 874–884.
25. Nolan, T., Deliyannis, G., Griffith, M., Braat, S., Allen, L.F., Audsley, J., Chung, A., Ciula, M., Gherardin, N., Giles, M., et al. (2023). Interim Results from a Phase I Trial of Novel SARS-CoV-2 Beta Variant Receptor-Binding Domain Recombinant Protein and mRNA Vaccines as a 4 th Dose Booster. https://doi.org/10.2139/ssrn.4485603.
26. Prevention, CfDCa (2024). COVID Data Tracker. https://covid.cdc.gov/covid-data-tracker/#trends_weeklydeaths_select_00:cdc.gov.
27. Wang, Q., Guo, Y., Zhang, R.M., Ho, J., Mohri, H., Valdez, R., Manthei, D.M., Gordon, A., Liu, L., and Ho, D.D. (2023). Antibody Neutralization of Emerging SARS-CoV-2: EG.5.1 and XBC.1.6. Preprint at bioRxiv. https://doi.org/10.1101/2023.08.21.553968.
28. Chalkias, S., McGhee, N., Whatley, J.L., Essink, B., Brosz, A., Tomassini, J.E., Girard, B., Wu, K., Edwards, D.K., Nasir, A., et al. (2023). Safety and Immunogenicity of XBB.1.5-Containing mRNA Vaccines. Preprint at medRxiv. https://doi.org/10.1101/2023.08.22.23293434.
29. Takanashi, A., Pouton, C.W., and Al-Wassiti, H. (2023). Delivery and Expression of mRNA in the Secondary Lymphoid Organs Drive Immune Responses to Lipid

Nanoparticle-mRNA Vaccines after Intramuscular Injection. Mol. Pharm. *20*, 3876–3885.

30. Pouton, C.W., Al-Wassiti, H., and Ho, J.K. (2022). Lipid nanoparticle formulation. PCT/AU2022/050913.
31. Akinc, A., Maier, M.A., Manoharan, M., Fitzgerald, K., Jayaraman, M., Barros, S., Ansell, S., Du, X., Hope, M.J., Madden, T.D., et al. (2019). The Onpattro story and the clinical translation of nanomedicines containing nucleic acid-based drugs. Nat. Nanotechnol. *14*, 1084–1087.
32. Schoenmaker, L., Witzigmann, D., Kulkarni, J.A., Verbeke, R., Kersten, G., Jiskoot, W., and Crommelin, D.J.A. (2021). mRNA-lipid nanoparticle COVID-19 vaccines: Structure and stability. Int. J. Pharm. *601*, 120586.
33. Mui, B.L., Tam, Y.K., Jayaraman, M., Ansell, S.M., Du, X., Tam, Y.Y.C., Lin, P.J., Chen, S., Narayanannair, J.K., Rajeev, K.G., et al. (2013). Influence of Polyethylene Glycol Lipid Desorption Rates on Pharmacokinetics and Pharmacodynamics of siRNA Lipid Nanoparticles. Mol. Ther. Nucleic Acids *2*, e139.
34. Al-Wassiti, H., and Pouton, C.W. (2019). Biodistribution of LNPs (unpublished work).
35. Cheng, Q., Wei, T., Farbiak, L., Johnson, L.T., Dilliard, S.A., and Siegwart, D.J. (2020). Selective organ targeting (SORT) nanoparticles for tissue-specific mRNA delivery and CRISPR-Cas gene editing. Nat. Nanotechnol. *15*, 313–320.
36. Dilliard, S.A., Cheng, Q., and Siegwart, D.J. (2021). On the mechanism of tissue-specific mRNA delivery by selective organ targeting nanoparticles. Proc. Natl. Acad. Sci. USA *118*, e2109256118.
37. Wang, X., Liu, S., Sun, Y., Yu, X., Lee, S.M., Cheng, Q., Wei, T., Gong, J., Robinson, J., Zhang, D., et al. (2023). Preparation of selective organ-targeting (SORT) lipid nanoparticles (LNPs) using multiple technical methods for tissue-specific mRNA delivery. Nat. Protoc. *18*, 265–291.
38. Tan, C.W., Chia, W.N., Qin, X., Liu, P., Chen, M.I.C., Tiu, C., Hu, Z., Chen, V.C.W., Young, B.E., Sia, W.R., et al. (2020). A SARS-CoV-2 surrogate virus neutralization test based on antibody-mediated blockage of ACE2-spike protein-protein interaction. Nat. Biotechnol. *38*, 1073–1078.
39. Kleanthous, H., Silverman, J.M., Makar, K.W., Yoon, I.K., Jackson, N., and Vaughn, D.W. (2021). Scientific rationale for developing potent RBD-based vaccines targeting COVID-19. NPJ Vaccines *6*, 128.
40. Zhang, N.N., Li, X.F., Deng, Y.Q., Zhao, H., Huang, Y.J., Yang, G., Huang, W.J., Gao, P., Zhou, C., Zhang, R.R., et al. (2020). A Thermostable mRNA Vaccine against COVID-19. Cell *182*, 1271–1283.e16.
41. Mulligan, M.J., Lyke, K.E., Kitchin, N., Absalon, J., Gurtman, A., Lockhart, S., Neuzil, K., Raabe, V., Bailey, R., Swanson, K.A., et al. (2020). Phase I/II study of COVID-19 RNA vaccine BNT162b1 in adults. Nature *586*, 589–593.
42. Akahata, W., Sekida, T., Nogimori, T., Ode, H., Tamura, T., Kono, K., Kazami, Y., Washizaki, A., Masuta, Y., Suzuki, R., et al. (2023). Safety and immunogenicity of SARS-CoV-2 self-amplifying RNA vaccine expressing an anchored RBD: A randomized, observer-blind phase 1 study. Cell Rep. Med. *4*, 101134.
43. Bloom, J.D., Beichman, A.C., Neher, R.A., and Harris, K. (2023). Evolution of the SARS-CoV-2 Mutational Spectrum. Mol. Biol. Evol. *40*, msad085.
44. Kaku, C.I., Starr, T.N., Zhou, P., Dugan, H.L., Khalifé, P., Song, G., Champney, E.R., Mielcarz, D.W., Geoghegan, J.C., Burton, D.R., et al. (2023). Evolution of antibody immunity following Omicron BA.1 breakthrough infection. Nat. Commun. *14*, 2751.
45. Yue, C., Song, W., Wang, L., Jian, F., Chen, X., Gao, F., Shen, Z., Wang, Y., Wang, X., and Cao, Y. (2023). ACE2 binding and antibody evasion in enhanced transmissibility of XBB.1.5. Lancet Infect. Dis. *23*, 278–280.
46. Dadonaite, B., Crawford, K.H.D., Radford, C.E., Farrell, A.G., Yu, T.C., Hannon, W.W., Zhou, P., Andrabi, R., Burton, D.R., Liu, L., et al. (2023). A pseudovirus system enables deep mutational scanning of the full SARS-CoV-2 spike. Cell *186*, 1263–1278.e20.
47. Haddox, H.K., Galloway, J.G., Dadonaite, B., Bloom, J.D., Matsen, F.A., and DeWitt, W.S. (2023). Jointly modeling deep mutational scans identifies shifted mutational effects among SARS-CoV-2 spike homologs. Preprint at bioRxiv. https://doi.org/10.1101/2023.07.31.551037.
48. Starr, T.N., Greaney, A.J., Stewart, C.M., Walls, A.C., Hannon, W.W., Veesler, D., and Bloom, J.D. (2022). Deep mutational scans for ACE2 binding, RBD expression, and antibody escape in the SARS-CoV-2 Omicron BA.1 and BA.2 receptor-binding domains. PLoS Pathog. *18*, e1010951.
49. Baiersdörfer, M., Boros, G., Muramatsu, H., Mahiny, A., Vlatkovic, I., Sahin, U., and Karikó, K. (2019). A Facile Method for the Removal of dsRNA Contaminant from In Vitro-Transcribed mRNA. Mol. Ther. Nucleic Acids *15*, 26–35.